6056 *Inorg. Chem.* **1993,** *32,* 6056-6066

Studies of Monosubstituted Compounds of Formula $M_2(NMe_2)_5X$ ($M{\equiv}M$), Where M = Mo and W and X = I, Alkyl, Aryl, and Diphenylphosphido, and the Bridged-1,1′-ferrocenyl Complex $W_2(NMe_2)_4(\mu\text{-}(C_5H_4)_2Fe)$

Hartmut Schulz, Kirsten Folting, John C. Huffman, William E. Streib, and Malcolm H. Chisholm*

Department of Chemistry and Molecular Structure Center, Indiana University,
Bloomington, Indiana 47405

Received April 29, 1993[⊗]

The reaction between $M_2(NMe_2)_6$ and Me_3SiI (1 equiv) in toluene at 22 °C leads to an equilibrium mixture of $M_2(NMe_2)_6$, $M_2(NMe_2)_5I$, and $M_2(NMe_2)_4I_2$ (*ca.* 1:5:1), where M = Mo and W. The reactions between $M_2(NMe_2)_6$ and Me_2SiI (2 equiv) in toluene yield the compound $M_2(NMe_2)_4I_2$ in *ca.* 85% isolated yield. The monoiodo compounds are also formed by the reactions between $M_2(NMe_2)_6$ and $M_2(NMe_2)_4I_2$ in toluene. In solution the $M_2(NMe_2)_4I_2$ compounds exist as a mixture of *gauche* and *anti* isomers in a *ca.* 1:2 ratio. We have characterized by single-crystal X-ray crystallography (i) *anti*-$W_2(NMe_2)_4I_2$, (ii) a crystalline sample containing a solid solution of $Mo_2(NMe_2)_5I$ (90%) and *anti*- and *gauche*-$Mo_2(NMe_2)_4I_2$; and (iii) $W_2(NMe_2)_5I$ which contains a 5% disorder. Crystal data: for $W_2(NMe_2)_4I_2$ at -179 °C, $a = 7.838(3)$ Å, $b = 7.706(2)$ Å, $c = 15.010(5)$ Å, $\beta = 103.48(1)°$, $Z = 2$, $d_{calcd} = 3.05$ g cm^{-3}, and space group $P2_1/n$; for $Mo_2(NMe_2)_5I$ at -178 °C, $a = 14.251(2)$ Å, $b = 18.031(2)$ Å, $c = 7.477(1)$ Å, $Z = 4$, $d_{calcd} = 1.86$ g cm^{-3}, and space group *Pmnb*; for $W_2(NMe_2)_5I$ at -171 °C, $a = 14.220(2)$ Å, $b = 18.179(2)$ Å, $c = 7.449(1)$ Å, $Z = 4$, $d_{calcd} = 2.47$ g cm^{-3}, and space group *Pmnb*. In each of the above there is a staggered ethane-like M_2N_5I or $M_2N_4I_2$ core with $W{\equiv}W$ distances = 2.29(1) Å, and W—I = 2.69(1) Å (average) and $Mo{\equiv}Mo$ distances = 2.21(1) Å and Mo—I = 2.70(1) Å, with M—N in the range 1.92–1.97 Å. The substitution behavior of the $M_2(NMe_2)_5I$ compounds has been investigated by metathetic reactions involving $ClMgCH_2Ph$, $LiCH_2SiMe_3$, LiMe, $KCH_2C_6H_4$-3-Me, $LiPPh_2$, $(LiC_5H_4)_2Fe$, vinyl lithium, $LiC{\equiv}CR$, where R = Bu^t and Ph, $SnMe_4$, $Sn(vinyl)_4$, and $AlMe_3$. The monosubstituted compounds $M_2(NMe_2)_5R$ were isolated and characterized for R = Me, CH_2Ph, *m*-$CH_2C_6H_4Me$, and PPh_2. Substitution of the M–I bond in reactions involving organolithium compounds requires the addition of $Me_2NCH_2CH_2NMe_2$ (TMEDA). Reactions employing alkynyl- and vinyllithium reagents gave intractable products. The compound $W_2(NMe_2)_5(PPh_2)$ was crystallographically characterized and shown to contain an ethane-like W_2N_5P core [W–W = 2.304(1) Å, W–N = 1.95 Å (average), and W–P = 2.43 Å] and a pyramidal phosphido ligand. Crystal data for $W_2(NMe_2)_5(PPh_2)$ at -174 °C: $a = 20.653(3)$ Å, $b = 46.774(5)$ Å, $c = 11.223(3)$ Å, $Z = 16$, $d_{calcd} = 1.895$ g cm^{-3}, and space group *Fdd*2. Reactions employing $(LiC_5H_4)_2$-Fe and $M_2(NMe_2)_5I$ did not yield tetranuclear ferrocenyl linked compounds but gave the bridged dinuclear complexes $M_2(NMe_2)_4(\mu\text{-}(C_5H_4)_2Fe)$. Crystal data for $W_2(NMe_2)_4(\mu\text{-}C_5H_4)_2Fe)$ at -155 °C: $a = 15.426(3)$ Å, $b = 16.664(3)$ Å, $c = 9.727(2)$ Å, $\alpha = 90.34(1)°$, $\beta = 107.52(1)°$, $\gamma = 65.24(1)°$, $Z = 4$, $d_{calcd} = 2.263$ g cm^{-3}, and space group $P\bar{1}$. Selected distances for the two independent molecules in the unit cell (averaged): W–W = 2.28(1) Å, W–C = 2.11–2.18 Å, W–N = 1.88–1.98 Å for the ethane-like *gauche* $W_2C_2N_4$ core, and Fe–C = 1.98–2.12 Å for the ferrocenyl group. The compounds $M_2(NMe_2)_5R$, where M = Mo and R = CH_2Ph and M = W and R = CH_2SiMe_3, react with Me_3SiI (1 equiv) in toluene at 22 °C to give the respective $M_2(NMe_2)_4(R)(I)$ compounds which exist mostly in the *gauche* 1,2-disubstituted form in solution. The compound $Mo_2(NMe_2)_4(CH_2Ph)I$ reacted with $LiCH_2SiMe_3$ in hexane/THF at 22 °C to give the mixed 1,2-diorganodimolybdenum compound $Mo_2(NMe_2)_4(CH_2Ph)(CH_2SiMe_3)$.

Introduction

There is now an extensive coordination chemistry for d^3–d^3 M_2^{6+} containing compounds (M = Mo and W) and, within this class, the ethane-like $X_3M{\equiv}MX_3$ compounds hold a unique position.[1] An important subgroup of the latter are 1,2-$M_2Cl_2(NMe_2)_4$ compounds[2] because the chloride ligands are readily replaced by a wide variety of other ligands, e.g. R where R = alkyl,[3] aryl,[4] benzyl,[4] alkoxide,[5] thiolate, etc.[6] One general group of compounds that is currently conspicuous by its absence is that of general formula M_2X_5Y. These compounds are surely intermediates in reactions involving M_2X_6 compounds where X is replaced by Y to give either $M_2X_4Y_2$ or M_2Y_6 compounds. However, in our earlier studies of the preparation of $M_2Cl_2(NMe_2)_4$ compounds from the reactions between $M_2(NMe_2)_6$ and Me_3SiCl (2 equiv) we found that the equilibrium shown in eq 1 did not favor the monochloro derivatives.[2a] Furthermore,

$$2M_2(NMe_2)_5Cl \rightleftarrows M_2(NMe_2)_6 + M_2Cl_2(NMe_2)_4 \quad (1)$$

the compounds $M_2Cl_2(NMe_2)_4$ are preferentially crystallized from the equilibrium mixture in eq 1, and by ^{1}H NMR spectroscopy the relative concentration of $M_2(NMe_2)_5Cl$ is always small relative to the other species present in solution.

We reasoned that analogous iodo compounds might be substitutionally less labile than their analogues based on (i) the

---

[⊗] Abstract published in *Advance ACS Abstracts,* November 1, 1993.

(1) (a) Cotton, F. A.; Walton, R. A. *Multiple Bonds Between Metal Atoms,* 2nd ed.; Oxford University Press: London, 1993; Chapter X. (b) Chisholm, M. H. *Acc. Chem. Res.* **1990,** *23,* 419.

(2) (a) Akiyama, M.; Chisholm, M. H.; Cotton, F. A.; Extine, M. W.; Murillo, C. A. *Inorg. Chem.* **1977,** *16,* 2407. (b) Chisholm, M. H.; Martin, J. D. *Inorg. Synth.* **1992,** *29,* 137.

(3) Chisholm, M. H.; Haitko, D. A.; Huffman, J. C. *J. Am. Chem. Soc.* **1981,** *103,* 4046.

(4) Chetcuti, M. H.; Chisholm, M. H.; Folting, K.; Haitko, D. A.; Huffman, J. C.; Janos, J. *J. Am. Chem. Soc.* **1983,** *105,* 1163.

(5) Chisholm, M. H.; Parkin, I. P.; Huffman, J. C.; Lobkovsky, E. M.; Folting, K. *Polyhedron* **1991,** *10,* 2839.

(6) Chisholm, M. H.; Parkin, I. P.; Huffman, J. C.; Streib, W. E. *J. Chem. Soc., Chem. Commun.* **1990,** 920.

0020-1669/93/1332-6056$04.00/0

Scheme I. Reactions Showing the Formation and Equilibria *involving* $M_2(NMe_2)_6$, $M_2(NMe_2)_5I$, and $M_2(NMe_2)_4I_2$ in Toluene Solutions

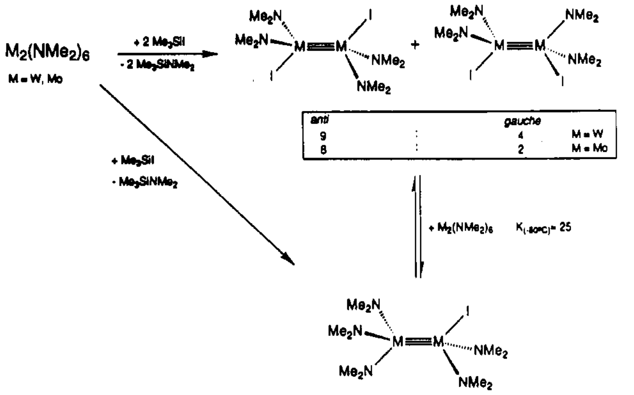

more covalent M–I bond and (ii) the greater size of the halide I > Cl.[7] This led us to examine the preparation of analogous iodo compounds and seek a synthetic route to $M_2(NMe_2)_5I$ compounds in order to investigate their substitution chemistry. We describe the results of these endeavors in this paper.

Results

Synthesis of $M_2(NMe_2)_4I_2$ and $M_2(NMe_2)_5I$. Addition of Me_3SiI (1 equiv) to a toluene solution of $M_2(NMe_2)_6$ at room temperature leads to an equilibrium mixture of $M_2(NMe_2)_6$, $M_2(NMe_2)_5I$, and $M_2(NMe_2)_4I_2$. When 2 equiv are added, $M_2(NMe_2)_4I_2$ is formed exclusively. For M = Mo a yellow-brown precipitate is formed upon addition of Me_3SiI that dissolves completely after stirring for several hours. The above mentioned equilibrium is also obtained by mixing $M_2(NMe_2)_4I_2$ and $M_2(NMe_2)_6$ (1:1) in toluene and stirring for about 6 h at room temperature. The reactions are summarized in Scheme I.

From integration of the ^1H NMR signals the equilibrium constant can be estimated to be $K(-85\ °C) = 25$; i.e., $M_2(NMe_2)_6$, $M_2(NMe_2)_5I$, and $M_2(NMe_2)_4I_2$ are present in a ratio of 1:5:1, respectively. Crystalline materials of almost pure $M_2(NMe_2)_5I$ are formed upon cooling a saturated toluene solution to −20 °C.

Reactions Involving $M_2(NMe_2)_5I$ with LiR (M = Mo, R = CH_2Ph; M = W, R = Me, CH_2SiMe_3, PPh_2), KR (M = W, R = *m*-$CH_2C_6H_4CH_3$), and ClMgR (M = W, R = CH_2Ph). The M–I bond is accessible to metathetic reactions with metallorganic compounds of formula LiR, KR, and ClMgR. However, the M–I bond exhibits a lower reactivity than the M–Cl bond in $M_2(NMe_2)_4Cl_2$ compounds. Whereas $M_2(NMe_2)Cl_2$ reacts, with LiR at room temperature.[3,4] $M_2(NMe_2)_5I$ compounds show no reaction unless $Me_2NCH_2CH_2NMe_2$ (TMEDA) is added to the solution. With $ClMgCH_2Ph$ or *m*-$KCH_2C_6H_4CH_3$ and $M_2(NMe_2)_5I$ a reaction is complete in less than 5 h.

Scheme II. Summary of Metathetic Reactions Involving $M_2(NMe_2)_5I$ Compounds Wherein $M_2(NMe_2)_5R$ Compounds are Formed

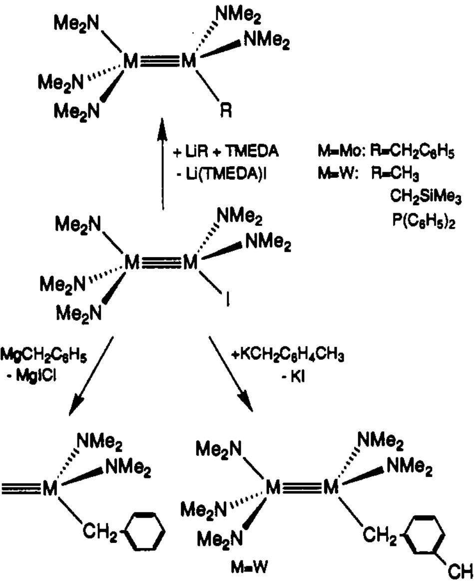

A general synthetic route to compounds of formula $M_2(NMe_2)_5R$ is as follows: slightly more than 1 equiv of LiR, KR, or ClMgR is dissolved in THF or Et_2O, and the solution is added to a toluene solution of $M_2(NMe_2)_5I$. In the case of LiR, TMEDA (slightly more than 1 equiv) is added to the $M_2(NMe_2)_5I$ solution before adding the lithium reagent. After the reaction mixture is stirred for several hours at room temperature, the solvent is removed under a dynamic vacuum. Then hexane is added, and the insoluble part (iodo salts or the Li(TMEDA)I complex) is removed by filtration. In addition to the desired product, the hexane fraction contains $M_2(NMe_2)_6$ as a major component. Separation is only achieved by fractional sublimation or distillation. At *ca* 120 °C and 10^{-3} Torr, $M_2(NMe_2)_6$ sublimes. The desired products distill as yellow-orange oils at slightly higher temperatures. Due to partial thermal decomposition ($T > 120$ °C) the isolated yields of the oily products are rather low. An exception is $W_2(NMe_2)_5PPh_2$, which is an orange crystalline solid at room temperature. It sublimes readily at 140-150 °C and 10^{-3} Torr, yielding pure product in *ca.* 60% yield based on tungsten.

Synthesis of $M_2(NMe_2)_4(R)R'$. $M_2(NMe_2)_5R$ compounds react with Me_3SiI (1 equiv) in toluene to yield $M_2(NMe_2)_4(R)I$. This was proven for M = Mo and R = CH_2Ph and M = W and R = CH_2SiMe_3. Both products are oily compounds that are difficult to purify because of considerable decomposition during distillation. Treatment of a toluene solution of $Mo_2(NMe_2)_4$-$(CH_2Ph)I$ with $LiCH_2SiMe_3$ (1 equiv) in THF results in the formation of the mixed dialkyl compound $Mo_2(NMe_2)_4$-$(CH_2PH)(CH_2SiMe_3)$. The compound is an oil at room temperature and exists almost exclusively in the *gauche* conformation as determined by NMR spectroscopic studies.

Reaction of $W_2(NMe_2)_5I$ with the Dilithio Compound $(LiC_5H_4)_2Fe$. The reaction of $W_2(NMe_2)_5I$ (2 equiv) with $(LiC_5H_4)_2Fe$ does not lead to the expected formation of a tetramer but to *gauche*-1,2-$W_2(NMe_2)_4(\mu$-$(C_5H_4)_2Fe)$. This 1,1′-ferrocenyl compound is a new derivative of the well-known class of compounds of general formula $M_2(NMe_2)_4R_2$. The $LiNMe_2$ formed during this cyclization reaction competes with remaining $(LiC_5H_4)_2Fe$ for the $W_2(NMe_2)_5I$ and forms $W_2(NMe_2)_6$. The reaction of $W_2(NMe_2)_5I$ with $LiNMe_2$ to yield $W_2(NMe_2)_6$ was shown in an independent experiment. The overall reaction pathway for the formation of *gauche*-1,2-$W_2(NMe_2)_4(\mu$-$(C_5H_4)_2Fe)$ is shown in Scheme III.

Reactions of $M_2(NMe_2)_5I$ with Vinyllithium and LiC≡CR (R = Ph, *t*-Bu). Reactions of $W_2(NMe_2)_5I$ with vinyllithium and LiC≡CR do not lead to any tractable products. This led us to believe that the amido ligands are involved in the above reactions. Indeed, $W_2(NMe_2)_6$ reacts with vinyllithium at room temperature in THF. Next to signals for excess starting materials ($W_2(NMe_2)_6$ or vinyllithium), only a single resonance at $\delta = 2.69$ (D_8-THF) is observed in the NMR tube experiment. This signal matches exactly that for $LiNMe_2$. The tungsten-containing reaction products are insoluble materials.

LiC≡CR does not show any reactivity toward $W_2(NMe_2)_6$. Therefore in $W_2(NMe_2)_5I$ the only reactive center should be the M–I bond leading to the formation of the metathesis products. A different triply bonded tungsten dimer $Cp'_2W_2Cl_4$ (Cp′ =

---

[7] The dibromo- and diiodo compounds $W_2X_2(NEt_2)_4$ had been prepared previously and structurally characterized: Chisholm, M. H.; Cotton, F. A.; Extine, M. W.; Millar, M.; Stults, B. R. *Inorg. Chem.* **1977**, *16*, 32. These *diethylamido* compounds are prepared in lower yields relative to dimethylamido compounds, presumably due to the greater steric hindrance $NEt_2 > NMe_2$ and have not been used in extensive synthetic work because of this fact.

Table I. Summary of Crystal Data[a]

	I	II	III	IV	V
empirical formula	$C_8H_{22}I_2N_4W_2$	$C_{10}H_{30}IN_5W_2$	$C_{10}H_{30}IMo_2N_5$	$C_{22}H_{40}N_5P_1W_2$	$C_{18}H_{32}Fe_1N_4W_2$
space group	$P2_1/n$	*Pmnb*	*Pmnb*	*Fdd*2	$P\bar{1}$
temp (°C)	–179	–171	–178	–174	–155
a (Å)	7.838(3)	14.220(2)	14.251(2)	20.653(1)	15.426(3)
b (Å)	7.706(2)	18.179(2)	18.031(2)	46.774(1)	16.664(3)
c (Å)	15.010(5)	7.449(1)	7.477(1)	11.223(1)	9.727(2)
α (deg)					90.34(12)
β (deg)	103.48(1)				107.52(1)
δ (deg)					65.24(1)
Z (molecules/cell)	2	4	4	16	4
V (Å^3)	881.63	1925.4	1921.26	10839.84	2144.53
calcd density (gm/cm^3)	3.0055	2.466	1.860	1.895	2.263
λ (Å)	0.710 69	0.710 69	0.710 69	0.710 69	0.710 69
MW	797.81	714.98	539.17	773.27	730.04
μ (cm^{-1})	335.539	137.806	28.559	87.410	116.215
2θ (deg)	6 – 45	6 – 55	6 – 50	6 – 55	6 – 45
R(*F*)[b]	.0388	.0471	.0346	.0520	.0611
$R_w(F)$[c]	.0416	.0450	.0369	.0494	.0603

[a] I = $W_2(NMe_2)_4I_2$; II = $W_2(NMe_2)_5I$; III = $Mo_2(NMe_2)_5I$ (90%), $Mo_2(NMe_2)_4I_2$ (10%); IV = $W_2(NMe_2)_5(PPh_2)$; V = $W_2(NMe_2)_4(\mu-(C_5H_4)_2Fe)$. [b] $R(F) = \Sigma(|F_o| - |F_c|)/\Sigma|F_o|$. [c] $R_w(F) = [\Sigma w(|F_o| - |F_c|)^2/\Sigma w|F_o^2/^{1/2}$.

Scheme III. Formation of $W_2(NMe_2)_4(\mu\text{-}(C_5H_4)_2Fe)$ in the Reaction between $W_2(NMe_2)_5I$ and $(LiC_5H_4)_2Fe$

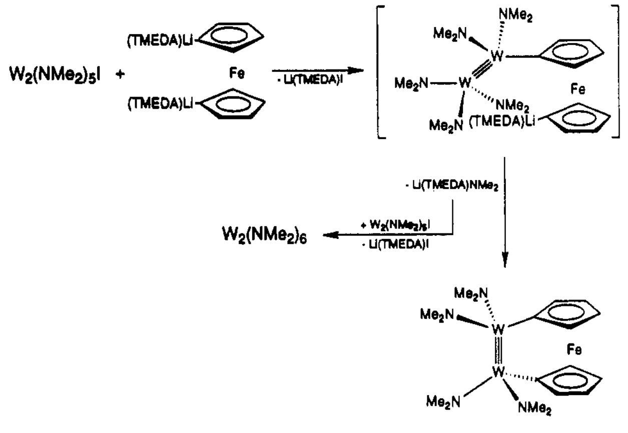

isopropanylcyclopentadienyl)[8] gives with LiC≡CR (R = Ph, *t*-Bu) only intractrable products although the Cp′ rings are expected to be relatively inert. It seem therefore that the triple bond takes part in the reaction and gives rise to different reaction pathways. Interestingly the quadruply bonded species $M_2X_4(PMe_3)_4$ (M = Mo, W; X = Cl, Br, I) are known to react in fairly good yields with LiC≡CR (R = Ph, *t*-Bu, $SiMe_3$) to yield the corresponding tetraacetylides.[9]

Reactivity of $M_2(NMe_2)_5I$ toward SnR_4 (R = Me, Vinyl) and $AlMe_3$. In organometallic chemistry tin and aluminum alkyl compounds are well-known to react as alkylating agents.[10] Therefore, their reactivity toward $M_2(NMe_2)_5I$ was investigated. With SnR_4 no reaction is observed even at higher temperatures. Both starting materials can be recovered. $AlMe_3$ reacts at low temperatures (–20 °C) to form intractable products. Presumably aluminum is capable of removing NMe_2 ligands as well as the iodide.

Solid-State and Molecular Structures

A summary of crystal data is given in Table I. Listings of atomic coordinates and isotropic thermal parameters are given in Tables II–VI for the five structural determinations of this work.

Table II. Fractional Coordinates and Isotropic Thermal Parameters for $W_2(NMe_2)_4I_2$

atom	10^4x	10^4y	10^4z	$10B_{iso}$ (Å^2)
W(1)	9563(1)	791(1)	554.5(4)	8
I(2)	7052(1)	2975(1)	–308(1)	13
N(3)	11687(14)	1928(16)	1185(8)	11
C(4)	13519(19)	1869(20)	1066(11)	16
C(5)	11573(20)	3002(22)	1971(10)	18
N(6)	8669(15)	–967(15)	1257(8)	11
C(7)	8549(17)	–2830(20)	1197(10)	15
C(8)	8090(20)	–351(21)	2045(12)	18

Table III. Fractional Coordinates and Isotropic Thermal Parameters for $W_2(NMe_2)_5I$

atom	10^4x	10^4y	10^4z	$10B_{iso}$ (Å^2)
W(1)	7500*	3098.1(3)	867(1)	15
W(2)	7500*	4357.5(3)	1126(1)	14
I(3)	7500*	2526(1)	4195(1)	27
N(4)	8646(6)	2905(5)	–424(13)	21
C(5)	9369(9)	3374(8)	–1237(18)	33
C(6)	8824(10)	2120(6)	–845(16)	30
N(7)	7500*	4705(7)	–1380(20)	20
C(8)	7500*	4336(10)	–3133(27)	35
C(9)	7500*	5514(9)	–1622(29)	33
N(10)	8643(7)	4572(5)	2413(13)	22
C(11)	9425(10)	4115(8)	3072(22)	38
C(12)	8815(12)	5358(7)	2873(23)	44
I(13)	9298(12)	4574(10)	2788(23)	29(3)
I(14)	7500*	4806(22)	–2471(61)	36(6)

Table IV. Fractional Coordinates and Isotropic Thermal Parameters for $Mo_2(NMe_2)_5I$

atom	10^4x	10^4y	10^4z	$10B_{iso}$ (Å^2)
Mo(1)	7500*	3122.7(4)	898(1)	15
Mo(2)	7500*	4344.5(4)	1153(1)	13
I(3)	7500*	2516.3(3)	4204(1)	27
N(4)	8649(4)	2925(3)	–381(7)	22
C(5)	8822(5)	2146(4)	–799(9)	31
C(6)	9366(5)	3393(4)	–1195(9)	33
N(7)	8650(4)	4563(3)	2459(7)	19
C(8)	8821(6)	5339(4)	2892(11)	32
C(9)	9417(5)	4109(5)	3123(11)	30
N(10)	7500*	4693(4)	–1292(11)	18
C(11)	7500*	5505(6)	–1547(14)	31
C(12)	7500*	4325(6)	–3021(13)	31
I(3A)	9300(8)	4580(7)	2855(15)	31(3)
I(3B)	7500*	4885(10)	–2278(29)	32(6)

$W_2(NMe_2)_4I_2$. An ORTEP drawing of the molecule is given in Figure 1 that shows the atom-numbering scheme used in the tables. In the space group $P2_1/n$ there is one unique molecule in the unit cell and this has a crystallographically imposed center of inversion. Selected bond distances and angles are given in Table VII.

$W_2(NMe_2)_5I$. An ORTEP drawing of the molecule is given in Figure 2. A selected list of bond distances and bond angles

---

(8) Green, M. L. H.; Mounford, P. P. *J. Chem. Soc. Rev.* **1992**, *21*, 29.
(9) Hopkins, M. D.; Stoner, T. C.; Dallinger, R. F. *J. Am. Chem. Soc.* **1990**, *112*, 5651.
(10) Elschenbroich, Ch.; Salzer, A. *Organometallics: A Concise Introduction*, 2nd ed., VCH Publishers: Weinheim, Germany, 1991.

Table V. Fractional Coordinates and Isotropic Thermal Parameters for $W_2(NMe_2)_5PPh_2$

atom	10^4x	10^4y	10^4z	$10B_{iso}$ (Å^2)	atom	10^4x	10^4y	10^4z	$10B_{iso}$ (Å^2)
W(1)	−932.5(2)	1777.7(1)	−6231*	9	N(16)	−1666(5)	1893(2)	−7214(9)	11
W(2)	−1158.9(2)	1980.1(1)	−4406(1)	11	C(17)	−1624(8)	−1808(3)	−8451(12)	17
P(3)	21(2)	2037(1)	−6901(3)	12	C(18)	−2288(7)	2034(3)	−6920(14)	14
C(4)	411(6)	1756(3)	−7818(11)	11	N(19)	−810(6)	1374(2)	−5906(11)	17
C(5)	344(7)	1772(3)	−9052(12)	16	C(20)	−790(8)	1198(3)	−4831(13)	19
C(6)	607(7)	1558(3)	−9803(12)	18	C(21)	−757(6)	1189(3)	−6963(12)	14
C(7)	926(7)	1331(3)	−9292(15)	21	N(22)	−1950(7)	1778(3)	−3903(14)	22
C(8)	1012(8)	1306(3)	−8070(13)	20	C(23)	−2236(8)	1862(4)	−2750(18)	31
C(9)	739(6)	1524(3)	−7337(11)	8	C(24)	−2359(7)	1577(3)	−4520(15)	21
C(10)	638(6)	2162(3)	−5852(12)	12	N(25)	−1295(6)	2385(3)	−4780(12)	18
C(11)	1297(6)	2079(3)	−5942(12)	14	C(26)	−1256(7)	2560(3)	−5864(14)	19
C(12)	1757(7)	2191(4)	−5198(15)	23	C(27)	−1527(9)	2563(3)	−3776(19)	28
C(13)	1570(6)	2393(3)	−4330(14)	19	N(28)	−415(6)	1895(3)	−3409(10)	18
C(14)	932(7)	2475(3)	−4224(11)	15	C(29)	175(6)	1731(3)	−3564(12)	14
C(15)	470(7)	2357(3)	−4986(14)	17	C(30)	−432(9)	2031(5)	−2185(16)	37

Table VI. Fractional Coordinates and Isotropic Thermal Parameters for $W_2(NMe_2)_4$ (μ-$(C_5H_4)_2Fe$)

atom	10^4x	10^4y	10^4z	$10B_{iso}$ (Å^2)	atom	10^4x	10^4y	10^4z	$10B_{iso}$ (Å^2)
W(1)A	4821(1)	3573(1)	2609(2)	11	W(1)B	1695(1)	1631(1)	8003(2)	10
W(2)A	3310(1)	3520(1)	1535(2)	11	W(2)B	278(1)	1828(1)	6119(2)	11
Fe(3)A	4963(4)	1676(4)	4031(5)	12	Fe(3)B	−338(4)	2235(3)	9184(5)	12
N(4)A	5621(23)	3029(20)	1316(32)	16(6)	N(4)B	2326(23)	416(20)	8750(32)	15(6)
C(5)A	5386(31)	2762(27)	−116(44)	24(7)	C(5)B	2191(30)	−408(27)	8374(43)	22(7)
C(6)A	6645(28)	2995(25)	1794(39)	15(7)	C(6)B	3294(32)	111(28)	10146(45)	25(8)
N(7)A	4482(19)	4827(17)	2794(27)	2(5)	N(7)B	2468(21)	1998(19)	7178(30)	12(5)
C(8)A	3577(29)	5643(26)	2215(41)	19(7)	C(8)B	2439(27)	2162(24)	5693(38)	12(6)
C(9)A	5342(24)	5029(22)	3428(35)	7(6)	C(9)B	3421(29)	1921(26)	8111(41)	19(7)
N(10)A	2456(26)	4103(24)	2723(37)	27(7)	N(10)B	−304(24)	3063(21)	5227(34)	20(6)
C(11)A	1480(28)	4086(25)	2192(39)	15(7)	C(11)B	−1289(26)	3366(23)	4069(36)	10(6)
C(12)A	2545(28)	4636(25)	3888(41)	18(7)	C(12)B	53(31)	3761(28)	5408(44)	24(7)
N(13)A	2832(23)	4102(20)	−455(32)	16(6)	N(13)B	731(22)	914(20)	4869(31)	14(6)
C(14)A	1903(31)	4150(28)	−1477(44)	24(7)	C(14)B	−53(25)	890(22)	3629(35)	8(6)
C(15)A	3155(28)	4644(25)	−1159(40)	19(7)	C(15)B	1713(33)	319(29)	4797(46)	28(8)
C(16)A	5264(26)	2760(23)	4617(36)	10(6)	C(16)B	867(30)	2495(27)	9302(42)	21(7)
C(17)A	4658(33)	2596(29)	5458(46)	28(8)	C(17)B	−66(26)	3332(23)	8858(37)	12(6)
C(18)A	5277(25)	1735(22)	6266(36)	9(6)	C(18)B	−507(29)	3397(26)	10006(41)	20(7)
C(19)A	6169(32)	1291(29)	5882(46)	27(8)	C(19)B	160(26)	2661(23)	11155(37)	12(6)
C(20)A	6185(32)	1973(28)	4947(44)	26(8)	C(20)B	999(33)	2111(29)	10683(46)	27(8)
C(21)A	4010(24)	2065(21)	1930(33)	5(6)	C(21)B	−473(25)	1554(23)	7407(36)	9(6)
C(22)A	4936(26)	1399(23)	2037(36)	11(6)	C(22)B	−157(28)	994(25)	8763(39)	16(7)
C(23)A	5193(30)	587(27)	2915(42)	21(7)	C(23)B	−891(28)	1317(25)	9431(39)	18(7)
C(24)A	4252(27)	825(25)	3375(39)	16(7)	C(24)B	−1668(27)	2154(24)	8584(38)	15(7)
C(25)A	3626(25)	1684(22)	2776(36)	8(6)	C(25)B	−1439(32)	2275(28)	7330(44)	24(7)

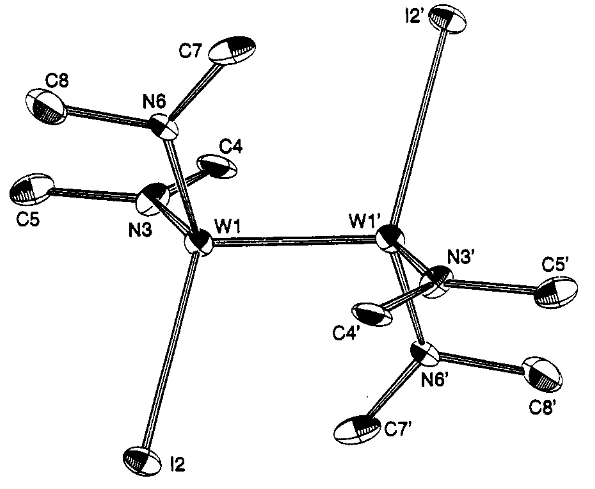

Figure 1. ORTEP drawing of the $W_2(NMe_2)_4I_2$ molecule giving the atom numbering scheme used in the tables.

are given in Table VIII. The molecule has a crystallographically imposed mirror plane of symmetry containing the W–W–I moiety. During the refinement it because apparent that there was a disorder problem associated with the molecule. This disorder was localized at W(2) such that a partial (5%) occupancy of I was present at each of the NMe_2 positions. This presumably reflects a solid solution or cocrystallization of $W_2(NMe_2)_5I$ and 5% *anti* + *gauche* (1:2) $W_2(NMe_2)_4I_2$.

Table VII. Selected Bond Distances (Å) and Bond Angles (deg) for $W_2(NMe_2)_4I_2$

	Bond Distances		
W(1)–W(1)′	2.2929(13)	N(3)–C(4)	1.488(18)
W(1)–I(2)	2.6821(12)	N(3)–C(5)	1.460(20)
W(1)–N(3)	1.924(11)	N(6)–C(7)	1.440(20)
W(1)–N(6)	1.945(12)	N(6)–C(8)	1.442(21)
	Bond Angles		
W(1)′–W(1)–I(2)	107.03(5)	W(1)–N(3)–C(4)	132.5(9)
W(1)′–W(1)–N(3)	103.2(3)	W(1)–N(3)–C(5)	116.5(9)
W(1)′–W(1)–N(6)	103.3(3)	C(4)–N(3)–C(5)	110.8(11)
I(2)–W(1)–N(3)	113.9(4)	W(1)–N(6)–C(7)	133.3(10)
I(2)–W(1)–N(6)	112.5(3)	W(1)–N(6)–C(8)	115.9(9)
N(3)–W(1)–N(6)	115.5(5)	C(7)–N(6)–C(8)	110.6(12)

$Mo_2(NMe_2)_5I$ (90%) and $Mo_2(NMe_2)_4I_2$ (10%). The solid-state structure revealed the presence of a solid solution of $Mo_2(NMe_2)_5I$ (90%) and roughly 5% each of *gauche*- and *anti*-$Mo_2(NMe_2)_4I_2$. The ORTEP drawings of the three molecules giving the atom number scheme used in the tables are given in Figures 3–5. Each molecule contains a crystallographically equivalent $Mo(NMe_2)_2I$ unit. The disorder of the other half of the molecule resembles that noted above for $W_2(NMe_2)_5I$. Selected bond distances and bond angles for $Mo_2(NMe_2)_5I$, *gauche*-$Mo_2(NMe_2)_4I_2$, and *anti*-$Mo_2(NMe_2)_4I_2$ are given in Table IX.

$W_2(NMe_2)_5(PPh_2)$. An ORTEP drawing of the molecule found in the solid state is given in Figure 6 and a view looking down the W-W axis and showing the pyramidal coordination at

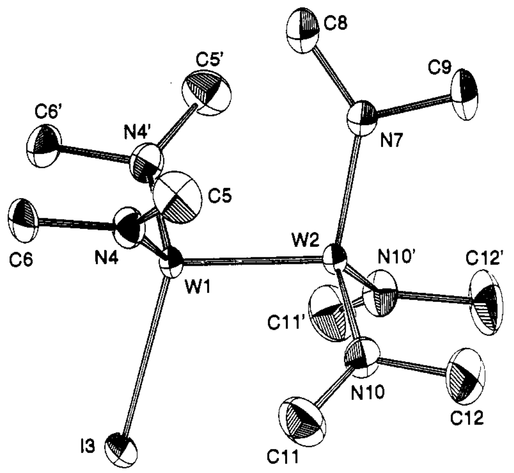

Figure 2. ORTEP drawing of the $W_2(NMe_2)_5I$ molecule showing the atom numbering scheme used in the tables.

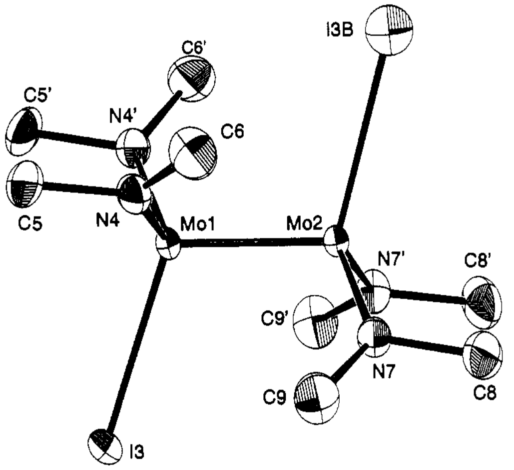

Figure 3. ORTEP drawing of the $Mo_2(NMe_2)_4I_2$ molecule showing the atom numbering scheme used in the tables.

Table VIII. Selected Bond Distances (Å) and Bond Angles (deg) for $W_2(NMe_2)_5I$

	Bond Distances		
W(1)–W(2)	2.2976(8)	W(2)–N(7)	1.971(15)
W(1)–I(3)	2.6884(12)	W(2)–N(10)	1.926(9)
W(1)–N(4)	1.924(9)	N–C(av)	1.477(28)
	Bond Angles		
W(2)–W(1)–I(3)	107.94(4)	W(1)–N(4)–C(6)	115.2(8)
W(2)–W(1)–N(4)	102.90(27)	C(5)–N(4)–C(6)	110.6(9)
I(3)–W(1)–N(4)	113.0(3)	W(2)–N(7)–C(8)	134.1(11)
N(4)–W(1)–N(4)′	115.7(6)	W(2)–N(7)–C(9)	115.6(11)
W(1)–W(2)–N(7)	103.9(4)	C(8)–N(7)–C(9)	110.2(14)
W(1)–W(2)–N(10)	104.07(28)	W(2)–N(10)–C(11)	133.6(8)
N(7)–W(2)–N(10)	114.0(3)	W(2)–N(10)–C(12)	116.6(8)
N(10)–W(2)–N(10)′	115.0(6)	C(11)–N(10)–C(12)	109.9(11)
N(10)–W(2)–N(10)′	115.0(6)		

phosphorus is given in Figure 7. Selected bond distances and bond angles are given in Table X.

$W_2(NMe_2)_4(\mu\text{-}(C_5H_4)_2Fe)$. In this compound, which displays $P\bar{1}$ symmetry, there are two crystallographically independent molecules that are chemically very similar. A view of one molecule is given in Figure 8 that shows the atom number scheme and a view looking down the W–W axis is given in Figure 9. Selected bond distances and bond angles for the two molecules, denoted as **A** and **B**, are given in Table XI.

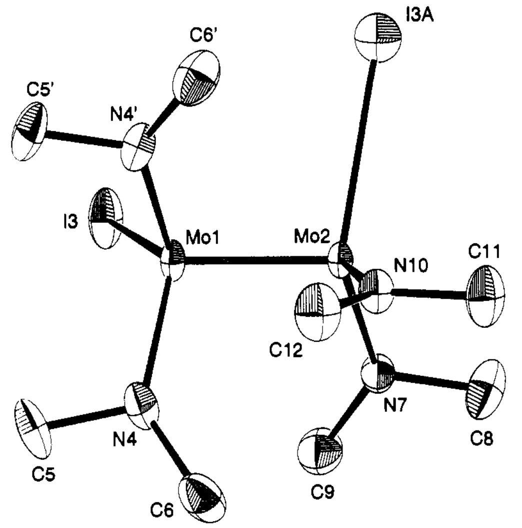

Figure 4. ORTEP drawing of the *gauche*-$Mo_2(NMe_2)_4I_2$ molecule giving the atom numbering scheme used in the tables. The equivalence of the NMe_2 groups attached to Mo(1) arises from the crystallographic disorder noted in the text.

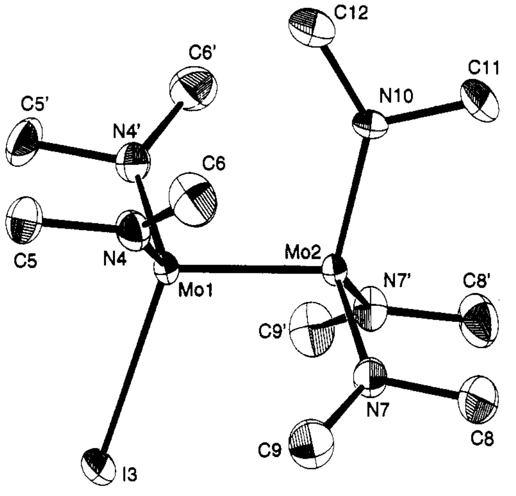

Figure 5. ORTEP dawing of the $Mo_2(NMe_2)_5I$ molecule giving the atom numbering scheme used in the tables.

Comments on the Molecular Structures. None of the structural parameters for the $M_2(NMe_2)_4I_2$ or $M_2(NMe_2)_5I$ compounds is exceptional based on our current knowledge of compounds of the form $M_2R_2(NMe_2)_4$.[3,4] The $W(NMe_2)_2(PPh_2)$ unit of $W_2(NMe_2)_5(PPh_2)$ closely resembles those seen in 1,2-$W_2(PPh_2)_2(NMe_2)_4$.[11] The pyramidal phosphorus atom is consistent with the relative π-donating power $NMe_2 > PPh_2$. However, it is worthy of mention that we did not observe bridge formation akin to that observed for $W_2(PPh_2)_2(NMe_2)_4 \rightleftarrows W_2(\mu\text{-}PPh_2)_2(NMe_2)_4$.[11] The bridged ferrocenyl compound is perhaps remarkable in that the 1,1′-ferrocenyl ligand is accommodated so readily by the *gauche*-$W_2(NMe_2)_4$ template.

Solution Behavior, NMR Studies

$M_2(NMe_2)_4I_2$. These compounds exist in a mixture of *anti* and *gauche* isomers. The M–N bonds show temperature-dependent rotations. At room temperature the signals are broad and badly resolved. At low temperatures, the rotations about the M–N bonds are frozen out and the proximal and distal methyl groups of both rotamers can be seen. In the *anti*-rotamer all four NMe_2 groups are identical and two signals in the ratio 1:1 for proximal and distal methyl groups are observed in both the ^1H and ^{13}C NMR spectra. In the *gauche* rotamer two sets of NMe_2 groups are present, and therefore four signals in the ratio 1:1:1:1 are detected. In *gauche*-$W_2(NMe_2)_4I_2$ the distal protons are accidentally degenerate and only three lines in the ratio 1:1:2 are observed. The ^{13}C NMR spectrum (−57 °C) of $W_2(NMe_2)_4I_2$ is shown in Figure 10.

---

(11) Buhro, W. E.; Chisholm, M. H.; Martin, J. D.; Folting, K.; Huffman, J. C.; Streib, W. E. *J. Am. Chem. Soc.* **1992**, *114*, 557.

Table IX. Selected Bond Distances (Å) and Bond Angles (deg) for $Mo_2(NMe_2)_5I^a$

Bond Distances			
I(3)–Mo(1)	2.7033(9)	N(4)–C(5)	1.461(8)
I(3A)–Mo(2)	2.895(12)	N(4)–C(6)	1.458(9)
I(3B)–Mo(2)	2.744(22)	N(7)–C(8)	1.457(8)
Mo(1)–Mo(2)	2.2112(10)	N(7)–C(9)	1.454(10)
Mo(1)–N(4)	1.929(5)	N(10)–C(11)	1.475(12)
Mo(2)–N(7)	1.947(5)	N(10)–C(12)	1.454(13)
Mo(2)–N(10)	1.933(9)		
Bond Angles			
I(3)–Mo(1)–Mo(2)	108.90(3)	N(7)–Mo(2)–N(7)	114.6(3)
I(3)–Mo(1)–N(4)	112.25(15)	N(7)–Mo(2)–N(10)	114.08(18)
Mo(2)–Mo(1)–N(4)	103.10(15)	Mo(1)–N(4)–C(5)	115.2(4)
N(4)–Mo(1)–N(4)	116.2(3)	Mo(1)–N(4)–C(6)	134.1(4)
I(3A)–Mo(2)–I(3B)	111.02(25)	C(5)–N(4)–C(6)	110.4(5)
I(3A)–Mo(2)–Mo(1)	100.63(25)	Mo(2)–N(7)–C(8)	116.6(4)
I(3A)–Mo(2)–N(7)	119.70(26)	Mo(2)–N(7)–C(9)	133.7(4)
I(3A)–Mo(2)–N(10)	111.58(23)	C(8)–N(7)–C(9)	109.8(5)
I(3B)–Mo(2)–Mo(1)	105.8(4)	Mo(2)–N(10)–C(11)	116.4(6)
I(3B)–Mo(2)–N(7)	113.37(22)	Mo(2)–N(10)–C(12)	133.8(6)
Mo(1)–Mo(2)–N(7)	104.19(15)	C(11)–N(10)–C(12)	109.7(8)
I(3A)–C(8)–N(7)	38.0(5)		

[a] Note: Because of the solid solution and disorder problem noted in the text and the supplementary materials, one should use caution in the interpretation of some of the distances and angles as in the case of "bond stretch isomerism": Yoon, K.; Parkin, G.; Rheingold, A. L. *J. Am. Chem. Soc.* **1992**, *114*, 2210. Parkin, G. *Chem. Rev.* **1993**, *93*, 887.

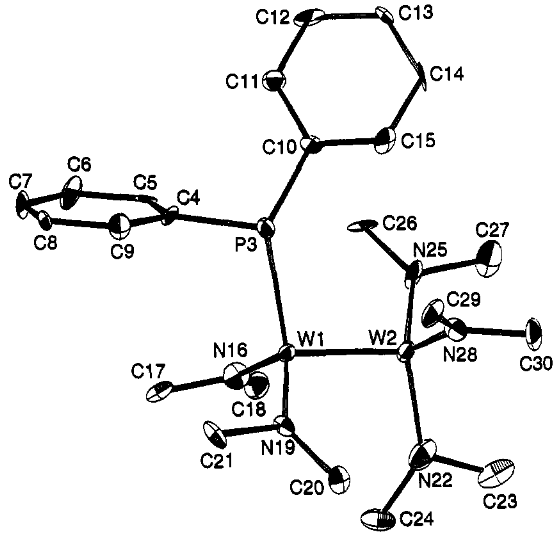

Figure 6. ORTEP drawing of the $W_2(NMe_2)_5(PPh_2)$ molecule giving the atom numbering scheme used in the tables.

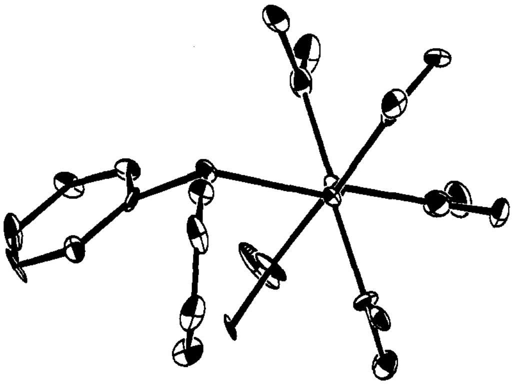

Figure 7. ORTEP drawing of the $W_2(NMe_2)_5(PPh_2)$ molecule looking down the W–W axis showing (i) the pyramidal coordination at phosphorus and (ii) the alignment of the NMe_2 groups to generate proximal and distal Me groups.

At higher temperatures one singlet for the *anti* rotamer and two singlets for the *gauche* rotamer should be present. At the high temperature limit also free rotation about the M–M triple bond should lead to only one singlet. However, even at 110 °C, the high-temperature limit of the solvent, the rotation about the M–N bond is not fast enough to lead to sharp lines in the ^1H NMR spectra. For $Mo_2(NMe_2)_4I_2$ only one broad signal is seen. In the case of $W_2(NMe_2)_4I_2$ the half-widths of the signals are somewhat smaller, and next to an intense broad signal, a rather sharp signal of lower intensity is present. This is attributed to one of the two expected signals for *gauche*-$W_2(NMe_2)_4I_2$ whereas the other one is hidden under the broad peak for the *anti* isomer. Obviously, at 110 °C, rotation about the M–M triple bond is still slow on the NMR time scale.

Table X. Selected Bond Distances (Å) and Bond Angles (deg) for $W_2(NMe_2)_5PPh_2$

Bond Distances			
W(1)–W(2)	2.3036(7)	W(2)–N(28)	1.942(11)
W(1)–P(3)	2.432(4)	P(3)–C(4)	1.855(13)
W(1)–N(16)	1.951(11)	P(3)–C(10)	1.830(14)
W(1)–N(19)	1.941(11)	N–C(av)	1.469(65)
W(2)–N(22)	1.972(14)	C–C(av)	1.395(49)
W(2)–N(25)	1.961(13)		
Bond Angles			
W(2)–W(1)–P(3)	103.55(9)	W(1)–N(16)–C(17)	114.8(10)
		W(1)–N(16)–C(18)	132.2(9)
W(2)–W(1)–N(16)	103.4(3)	C(17)–N(16)–C(18)	112.8(11)
W(2)–W(1)–N(19)	105.0(4)	W(1)–N(19)–C(20)	134.9(10)
P(3)–W(1)–N(16)	108.4(3)	W(1)–N(19)–C(21)	115.5(9)
P(3)–W(1)–N(19)	116.0(4)	C(20)–N(19)–C(21)	109.5(11)
N(16)–W(1)–N(19)	118.5(5)	W(2)–N(22)–C(23)	117.0(12)
W(1)–W(2)–N(22)	103.0(4)	W(2)–N(22)–C(24)	131.4(11)
W(1)–W(2)–N(25)	103.6(4)	C(23)–N(22)–C(24)	111.2(13)
W(1)–W(2)–N(28)	105.5(3)	W(2)–N(25)–C(26)	135.0(10)
N(22)–W(2)–N(25)	114.0(5)	W(2)–N(25)–C(27)	115.2(11)
N(22)–W(2)–N(28)	113.1(6)	C(26)–N(25)–C(27)	109.7(12)
N(25)–W(2)–N(28)	115.8(5)	W(2)–N(28)–C(29)	134.8(9)
W(1)–P(3)–C(4)	99.8(4)	W(2)–N(28)–C(30)	114.7(9)
W(1)–P(3)–C(10)	121.6(4)		
C(4)–P(3)–C(10)	106.2(6)		

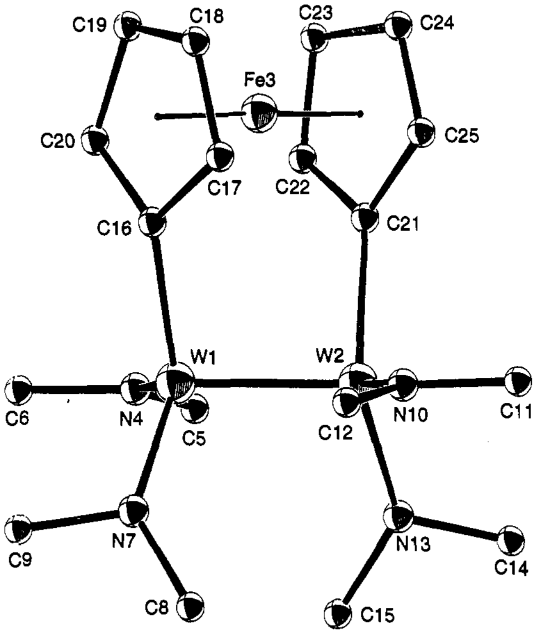

Figure 8. Ball-and-stick drawing of the $W_2(NMe_2)_4(\mu\text{-}(C_5H_4)_2Fe)$ molecule giving the atom number scheme used in the tables.

$M_2(NMe_2)_5X$, Where X = I or R. These compounds show similar variable-temperature NMR behavior that is consistent with expectations based on (i) M–N bond rotations that are slow or fast on the NMR time scale as a function of temperature and (ii) a frozen out M_2N_5X core; i.e., rotation about the M–M bond is always slow on the NMR time scale. At room temperature typically five signals are observed in the ^1H NMR spectrum for the NMe_2 groups corresponding to two NMe_2 groups that have frozen out proximal and distal methyl signals (presumably those (associated with the $M(NMe_2)_2X$ moiety) and two singlets in the

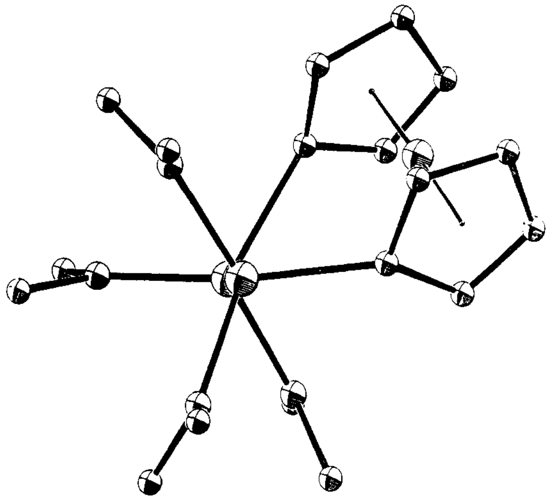

Figure 9. Ball-and-stick drawing of the $W_2(NMe_2)_4(\mu\text{-}(C_5H_4)_2Fe)$ molecule looking down the W–W axis.

ratio 2:1 corresponding to the *syn*- and *anti*-NMe_2 groups of the $M(NMe_2)_3$ moiety that are rotating rapidly at 22 °C.

At the low temperature limit six signals are expected for the five NMe_2 groups corresponding to proximal and distal methyl groups of three different types of NMe_2 ligands. The high temperature limiting spectra should show three lines in the ratio 2:2:1. This ideal behavior is exhibited best by $Mo_2(NMe_2)_5CH_2Ph$. The other $M_2(NMe_2)_5X$ compounds show deviations due to different rotation barriers of the M–N bonds. Also accidental degeneracy of the *syn* and *anti* NMe_2 groups can occur. Even at 100 °C, the anticipated high-temperature limiting spectra of three peaks in a ratio 2:2:1 is not fully obtained for any of the compounds.

For $M_2(NMe_2)_5I$ at high and low temperatures the spectra are complicated due to the signals of $M_2(NMe_2)_6$ and $M_2(NMe_2)_4I_2$. At room temperature the resonances for both $M_2(NMe_2)_6$ and $M_2(NMe_2)_4I_2$ are broad (compared to the signals of $M_2(NMe_2)_5I$) and are almost in the base line.

For $M_2(NMe_2)_5I$ the three different rotation barriers were calculated from the experimental data obtained by the variable-temperature measurements.[12] For both M = Mo and M = W the results are very similar. There is one set of two NMe_2 groups that show a rather high rotational barrier ($\Delta G^{\ddagger} = 16.7 \pm 0.4$ kcal/mol). This set is attributed to the NMe_2 groups of the $M(NMe_2)_2I$ moiety. The other two rotation barriers observed differ only little with the barrier for the *anti* NMe_2 groups *ca.* 1 kcal/mol higher in energy ($\Delta G^{\ddagger} = 10.2 \pm 0.5$ kcal/mol) than the barriers for the *syn* NMe_2 groups ($\Delta G^{\ddagger} = 9.2 \pm 0.4$ kcal/mol).

The ^{13}C NMR results are in total agreement with the ^1H NMR spectra discussed above. In addition to the signals for the common $M_2(NMe_2)_5$ moiety each compound of type $M_2(NMe_2)_5R$ shows the appropriate signals for the R groups. NMR active nuclei in the vicinity of tungsten couple to ^{183}W (14% natural abundance, $I = {}^1/_2$) giving rise to satellites in addition to the main signal of the spectra. The coupling constants of the methylene hydrogens in $W_2(NMe_2)_5R$ (R = CH_2Ph, CH_2SiMe_3, *m*-$CH_2C_6H_4CH_3$) span the range of $^2J(^{183}W\text{–}H) = 11.2\text{–}12.1$ Hz. $W_2(NMe_2)_5Me$ shows a smaller coupling of $^2J(^{183}W\text{–}H) = 8.7$ Hz. The ^{183}W–^{13}C coupling was detected only for $W_2(NMe_2)_5CH_2Ph$ and has a value of $^1J(^{183}W\text{–}^{13}C) = 91.4$ Hz. In $W_2(NMe_2)_5PPh_2$ the coupling between tungsten and phosphorus is $^1J(^{183}W\text{–}^{31}P) = 234.5$ Hz. All chemical shifts and coupling constants are in an expected range and similar to those seen in compounds of formula $M_2(NMe_2)_4R_2$.[3,4,11] The room-temperature ^1H NMR spectrum of $W_2(NMe_2)_5CH_2Ph$ is shown in Figure 11.

$W_2(NMe_2)_4(\mu\text{-}(C_5H_4)_2Fe)$. In the low-temperature limiting ^1H NMR spectra eight singlets are observed in the ratio 1:1:1:3:3:1:3:3. This is consistent with a ferrocenyl-bridged ethane-like tungsten dimer with four additional NMe_2 groups in the *gauche* configuration. The molecule has C_2 symmetry, *i.e.*, no mirror plane. Hence there are two sets of NMe_2 groups and one set of cyclopentadienyl groups. All four protons of each Cp ligand are chemically different and give rise to four singlets. The two sets of NMe_2 groups appear as another four singlets for proximal and distal methyl groups. When the compound is heated the M–N bonds start to rotate freely. One set of NMe_2 groups appears to have a considerably higher rotation barrier than the other. At room temperature the signals for these groups still give rise to two rather sharp singlets whereas the resonances for the other set are hidden in the base line. At 110 °C one set appears as a singlet and the other just emerges out of the base line as a broad hump. The protons on the Cp ligands show only a slight temperature shift over the whole temperature range indicating that there is no gauche to gauche enantiomerization via an eclipsed intermediate.

The ^{13}C NMR data are in full agreement with the ^1H NMR data discussed above. At low temperature four signals of equal intensity are observed for the NMe_2 groups and at room temperature only two are observed. In addition, there are five resonances for the Cp carbons.

$W_2(NMe_2)_4(CH_2SiMe_3)I$. At −57 °C several signals for proximal and distal methyl groups of the NMe_2 groups are observed that are due to the *gauche* isomer and presumably some *anti* isomer. Because of the lack of any symmetry element other than C_1, eight lines for the *gauche* and four lines for the *anti* isomer should be present. Characteristic, however, are the resonances of the methylene protons of CH_2SiMe_3. The methylene protons of the *gauche* rotamer are diastereotopic and give rise to two doublets of intensity 1:1 with the coupling constants $^2J(H\text{–}H) = 12.9$ Hz and $^2J(^{183}W\text{–}H) = 11.3$ Hz.

$Mo_2(NMe_2)_4(CH_2Ph)(CH_2SiMe_3)$. This compound also exists almost exclusively in the *gauche* conformation and shows at −67 °C eight singlets for the methyl resonances of the NMe_2 groups. The protons of both the methylene groups of CH_2Ph and CH_2SiMe_3 are diastereotopic and give rise to two doublets each. The resonances for the benzyl methylene protons are at $\delta = 3.82$ (d) and 3.44 (d) with $^2J(H\text{–}H) = 11.3$ Hz. The signals for the methylene protons of CH_2SiMe_3 are shifted upfield to $\delta = 1.64$ (d) and 1.24 (d) with $^2J(H\text{–}H) = 12.5$ Hz.

The ^{13}C NMR spectra are in full agreement with the ^1H NMR data. At −67 °C, eight lines are observed for the NMe_2 groups. The methylene carbons were assigned by running a DEPT experiment.

Concluding Remarks

The monoiodo compounds $M_2(NMe_2)_5I$ that are formed in the reactions between $M_2(NMe_2)_6$ and Me_3SiI in toluene are favored on thermodynamic grounds with respect to disproportionation to $M_2(NMe_2)_6$ and $M_2(NMe_2)_4I_2$ compounds. The M–I bond is labile to substitution and this has led to the first syntheses of $M_2(NMe_2)_5R$ compounds where R = an alkyl, a benzyl, and a phosphido ligand. The M–I for M–R exchange reaction is kinetically slower than the related substitutions of M–Cl bonds. Reactions employing certain organolithium and magnesium reagents, notably those where R = vinyl and acetylide, do not lead to simple substitution of the M–I bond, and intractable products are obtained. The lability of the M–NMe_2 bonds toward metathetic reactions is also seen in that reactions employing 1,1′-$Li_2(C_5H_4)_2Fe$ and $M_2(NMe_2)_5I$ always yield the bridged dinuclear compound $M_2[\mu\text{-}(C_5H_4)_2Fe](NMe_2)_4$ in preference to linked tetranuclear compounds. The further reaction between $M_2(NMe_2)_5R$ compounds with Me_3SiI (1 equiv) has led to the 1,2-$M_2(NMe_2)_4(R)(I)$ compounds which in turn are substitutionally labile and have allowed the first syntheses of mixed 1,2-dialkyl

---

[12] The $\Delta G^{\ddagger}$ values are determined from the observed coalescence temperatures: Pople, J. A.; Schneider, W. G.; Burnstein, H. J. *High Resolution NMR Spectroscopy*, McGraw-Hill: New York, 1959; p 223.

Table XI. Selected Bond Distances (Å) and Bond Angles (deg) for the Two Crystallographically Independent Molecules of $W_2(NMe_2)_4(\mu\text{-}(C_5H_4)_2Fe)$

	molecule A	molecule B		molecule A	molecule B
		Bond Distances			
W(1)–W(2)	2.2877(21)	2.2891(21)	Fe(3)–C(19)	2.03(4)	2.08(3)
W(1)–N(4)	1.98(3)	1.88(3)	Fe(3)–C(20)	2.09(4)	2.06(4)
W(1)–N(7)	1.953(25)	1.906(27)	Fe(3)–C(21)	2.04(3)	2.07(3)
W(1)–C(16)	2.14(3)	2.17(4)	Fe(3)–C(22)	1.98(3)	2.02(4)
W(2)–N(10)	1.96(3)	1.95(3)	Fe(3)–C(23)	2.07(4)	2.08(4)
W(2)–N(13)	1.95(3)	1.97(3)	Fe(3)–C(24)	2.12(4)	2.02(4)
W(2)–C(21)	2.18(3)	2.11(3)	Fe(3)–C(25)	2.05(3)	2.05(4)
Fe(3)–C(16)	2.08(3)	2.05(4)	N–C(av)	1.45(8)	1.47(16)
Fe(3)–C(17)	2.06(4)	2.08(3)	C–C(av)	1.44(15)	1.44(10)
Fe(3)–C(18)	2.09(3)	2.04(4)			
		Bond Angles			
W(2)–W(1)–N(4)	104.6(9)	105.5(9)	C(22)–Fe–(3)–C(25)	66.5(13)	68.5(16)
W(2)–W(1)–N(7)	105.6(7)	105.8(8)	C(23)–Fe(3)–C(24)	43.1(14)	41.1(14)
W(2)–W(1)–C(16)	97.6(9)	94.6(11)	C(23)–Fe(3)–C(25)	68.0(14)	67.7(15)
N(4)–W(1)–N(7)	116.7(11)	114.1(12)	C(24)–Fe(3)–C(25)	37.8(13)	40.4(15)
N(4)–W(1)–C(16)	115.4(13)	113.9(13)	W(1)–N(4)–C(5)	133.9(25)	137.8(25)
N(4)–W(1)–C(16)	113.9(11)	119.4(13)	W(2)–N(4)–C(6)	114.5(22)	115.9(23)
W(1)–W(2)–N(10)	106.6(10)	105.4(9)	C(5)–N(4)–C(6)	111(3)	106(3)
W(1)–W(2)–N(13)	105.0(9)	106.3(9)	W(1)–N(7)–C(8)	133.9(22)	133.6(22)
W(1)–W(2)–C(21)	92.5(8)	96.2(9)	W(1)–N(7)–C(9)	115.4(19)	118.1(22)
N(10)–W(2)–N(13)	115.8(14)	115.8(13)	C(8)–N(7)–C(9)	109.6(25)	106.6(26)
N(10)–W(2)–C(21)	114.3(13)	115.9(13)	W(2)–N(10)–C(11)	112.4(25)	114.7(22)
N(13)–W(2)–C(21	118.4(12)	114.3(12)	W(2)–N(10)–C(12)	133.4(26)	133.6(26)
C(16)–Fe(3)–C(17)	42.9(15)	41.6(15)	C(11)–N(10)–C(12)	114(3)	112(3)
C(16)–Fe(3)–C(18)	68.2(13)	69.5(15)	W(2)–N(13)–C(14)	119.8(23)	115.9(22)
C(16)–Fe(3)–C(19)	70.3(15)	68.8(14)	W(2)–N(13)–C(15)	132.3(24)	133.4(25)
C(16)–Fe(3)–C(20)	39.8(15)	40.1(15)	C(14)–N(13)–C(15)	107(3)	110(3)
C(16)–Fe(3)–C(21)	105.1(13)	103.9(14)	W(1)–C(16)–Fe(3)	105.2(15)	108.2(17)
C(16)–Fe(3)–C(22)	115.5(13)	115.1(15)	W(1)–C(16)–C(17)	132.1(27)	130.3(27)
C(16)–Fe(3)–C(23)	149.6(14)	149.2(16)	W(1)–C(16)–C(20)	115.6(25)	118(3)
C(16)–Fe(3)–C(24)	164.4(14)	166.0(15)	Fe(3)–C(16)–C(17)	67.9(20)	70.5(20)
C(16)–Fe(3)–C(25)	128.4(14)	126.8(16)	Fe(3)–C(16)–C(20)	70.3(22)	70.5(23)
C(17)–Fe(3)–C(18)	39.8(15)	41.3(14)	C(17)–C(16)–C(20)	106(3)	109(3)
C(17)–Fe(3)–C(19)	70.1(17)	69.2(13)	Fe(3)–C(17)–C(16)	69.2(21)	67.9(20)
C(17)–Fe(3)–C(20)	69.0(17)	68.7(15)	Fe(3)–C(17)–C(18)	71.1(23)	67.5(20)
C(17)–Fe(3)–C(21)	116.6(15)	114.0(13)	C(16)–C(17)–C(18)	106(3)	106(3)
C(17)–Fe(3)–C(22)	150.2(16)	148.7(14)	Fe(3)–C(18)–C(17)	69.1(22)	71.2(21)
C(17)–Fe(3)–C(23)	166.5(16)	169.1(14)	Fe(3)–C(18)–C(19)	67.4(21)	71.1(21)
C(17)–Fe(3)–C(24)	126.2(15)	128.7(14)	C(17)–C(18)–C(19)	112(3)	110(3)
C(17)–Fe(3)–C(25)	108.3(15)	106.6(15)	Fe(3)–C(19)–C(18)	72.1(22)	67.9(20)
C(18)–Fe(3)–C(19)	40.5(15)	41.0(14)	Fe(3)–C(19)–C(20)	71.2(23)	69.0(22)
C(18)–Fe(3)–C(20)	67.0(14)	68.7(16)	C(18)–C(19)–C(20)	105(3)	107(3)
C(18)–Fe(3)–C(21)	151.9(13)	149.6(15)	Fe(3)–C(20)–C(16)	69.9(22)	69.4(23)
C(18)–Fe(3)–C(22)	168.2(14)	168.6(15)	Fe(3)–C(20)–C(19)	66.9(22)	70.2(22)
C(18)–Fe(3)–C(23)	129.9(14)	132.1(15)	C(16)–C(20)–C(19)	110(3)	110(4)
C(18)–Fe(3)–C(24)	110.6(13)	109.7(15)	W(2)–C(21)–Fe(3)	107.7(14)	107.9(15)
C(18)–Fe(3)–C(25)	120.9(13)	118.1(16)	W(2)–C(21)–C(22)	135.5(24)	135.1(26)
C(19)–Fe(3)–C(20)	41.9(16)	40.8(15)	W(2)–C(21)–C(25)	115.5(22)	115.4(24)
C(19)–Fe(3)–C(21)	165.3(15)	165.7(14)	Fe(3)–C(21)–C(22)	67.9(19)	67.7(19)
C(19)–Fe(3)–C(22)	128.7(16)	129.2(14)	Fe(3)–C(21)–C(25)	69.9(18)	68.8(21)
C(19)–Fe(3)–C(23)	106.8(17)	111.3(14)	C(22)–C(21)–C(25)	104.5(28)	105(3)
C(19)–Fe(3)–C(24)	119.7(16)	120.3(14)	Fe(3)–C(22)–C(21)	72.5(19)	70.9(20)
C(19)–Fe(3)–C(25)	152.3(15)	152.8(15)	Fe(3)–C(22)–C923)	72.2(21)	72.7(22)
C(20)–Fe(3)–C(21)	126.1(14)	126.0(15)	C(21)–C(22)–C(23)	114(3)	111(3)
C(20)–Fe(3)–C(22)	108.1(15)	107.5(16)	Fe(3)–C(23)–C(22)	66.1(21)	67.9(21)
C(20)–Fe(3)–C(23)	118.0(16)	119.3(16)	Fe(3)–C(23)–C(24)	70.3(21)	67.0(20)
C(20)–Fe(3)–C(24)	155.3(16)	153.5(15)	C(22)–C(23)–C(24)	102(3)	107(3)
C(20)–Fe(3)–C(25)	165.1(15)	164.6(16)	Fe(3)–C(24)–C(23)	66.6(20)	71.9(21)
C(21)–Fe(3)–C(22)	39.6(13)	41.4(14)	Fe(3)–C(24)–C(25)	68.4(20)	71.0(22)
C(21)–Fe(3)–C(23)	69.8(14)	68.3(13)	C(23)–C(24)–C(25)	105(3)	108(3)
C(21)–Fe(3)–C(24)	68.3(13)	69.4(14)	Fe(3)–C(25)–C(21)	69.2(18)	70.0(21)
C(21)–Fe(3)–C(25)	40.9(12)	41.3(15)	Fe(3)–C(25)–C(24)	73.8(21)	68.6(21)
C(22)–Fe(3)–C(23)	41.7(14)	39.4(14)	C(21)–C(25)–C(24)	114(3)	109(3)
C(22)–Fe(3)–C(24)	69.0(14)	68.5(15)			

compounds 1,2-$M_2(NMe_2)_4(R)(R')$. The further utility of the monosubstituted compounds $M_2(NMe_2)_5I$ will be described elsewhere. They provide a useful entry point in the further development of the chemistry of $(M{\equiv}M)^{6+}$-containing compounds.

Experimental Section

All manipulations were carried out under an inert gas atmosphere (nitrogen or argon) with exclusion of air and moisture. All solvents were dried using standard methods and stored under inert gas. Elemental analyses were performed by Oneida Research Services. ^1H and ^{13}C NMR data were recorded on a Varian XL-300. The protio impurities in the deuterated solvents were used as internal standards and related to tetramethylsilane. ^{31}P NMR data were recorded on a Nicolet NT-360 using H_3PO_4 (85%) as external standard. The mass spectroscopical data were recorded on a Kratos MS-80.

The following compounds have been prepared according to the literature: $W_2(NMe_2)_6$,[13] $Mo_2(NMe_2)_6$,[14] *m*-$KCH_2(C_6H_4)CH_3$,[15] $Li_2[Fe(C_5H_4)_2]$.[16]

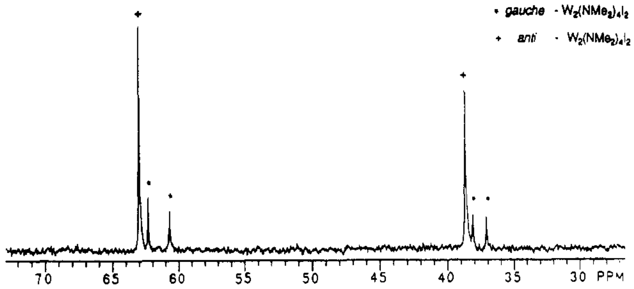

Figure 10. $^{13}C\{^1H\}$ NMR spectrum of $W_2(NMe_2)_4I_2$ at −57 °C, 75 MHz, in toluene-d_8 showing the presence of the *anti* and *gauche* rotamers.

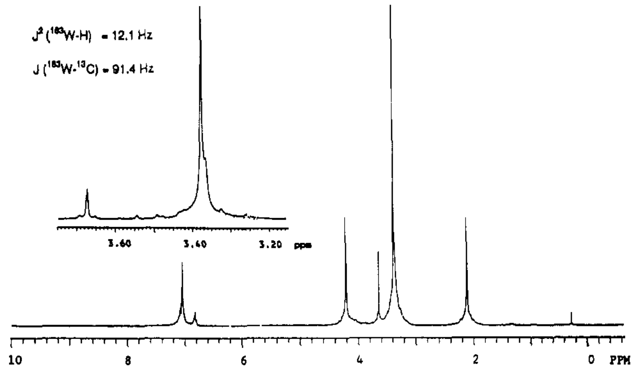

Figure 11. Room-temperature ^1H NMR spectrum of $W_2(NMe_2)_5(CH_2Ph)$ recorded in benzene-d_6 at 300 MHz.

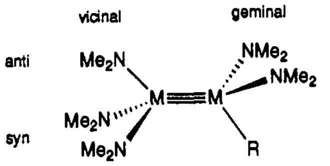

Figure 12. Notation used to describe the NMe_2 groups in $M_2(NMe_2)_5R$ compounds.

The NMe_2 groups are distinguished by their relative position to R as indicated in Figure 12.

Preparation of $M_2(NMe_2)_4I_2$ (M = Mo, W). A solution of 8.25 mmol of Me_3SiI in 40 mL of toluene was added to a solution of 4.12 mmol of $M_2(NMe_2)_6$ in 80 mL of toluene at room temperature over a period of 30 min. For M = Mo a yellow precipitate was formed upon addition that dissolved completely after several hours. The brown-red solution was stirred for 24 h. The reaction mixture was filtered through a fine frit, and the solvent was removed in *vacuo*. The brown-orange solid residue was washed twice with 20 mL of hexane and dried under vacuum at 40 °C for 3 h. Crystalline material was obtained from a saturated toluene solution at −20 °C. Yield: *ca.* 3.5 mmol = 85%.

Characterization Data for $W_2(NMe_2)_4I_2$. Properties: orange crystals, soluble in toluene and THF and insoluble in saturated hydrocarbons; mp >160 °C dec. Anal. Calcd for $C_8H_{24}I_2W_2$ (M_r 797.62): C, 12.05; H, 3.01; N, 7.02. Found: C. 12.05; H, 2.95; N, 7.03. NMR data (^1H, 299.94 MHz; ^{13}C, 75.43 MHz; toluene-d_8): ^1H (−58 °C) $\delta = 4.16$ and 2.23 (ratio of integrals 1:1, *anti*-$W_2(NMe_2)_4I_2$), 4.14, 3.72 and 2.16 (ratio of integrals 1:1:2, *gauche*-$W_2(NMe_2)_4I_2$) ratio of *anti*/*gauche* ≈ 9:4; ^1H (22 °C) $\delta = 4.15$ and 2.3 (broad, *anti*-$W_2(NMe_2)_4I_2$), 3.85 and 2.30 (*gauche*-$W_2(NMe_2)_4I_2$); ^1H (100 °C) $\delta = 3.27$ (broad), 3.14; ^{13}C (−58 °C) $\delta = 63.01$ and 38.66 (*anti*) 62.35, 60.71, 38.12 and 37.10 (*gauche*); ^{13}C (−17 °C) $\delta = 60.59$ (broad), 37.58 (broad). MS (EI): $m/z = 797$ ($M^+ - H$, 0.5%), 44 (NMe_2^+, 100%).

Characterization Data for $Mo_2(NMe_2)_4I_2$. Properties: orange solid, soluble in toluene and THF and insoluble in saturated hydrocarbons; mp >150 °C dec. Anal. Calcd for $C_8H_{24}I_2N_4Mo_2$ (M_r 621.80): C, 15.45; H, 3.86; N, 9.01. Found: C, 15.56; H, 3.90; N, 8.39. NMR data (^1H, 299.94 MHz, ^{13}C, 75.43 MHz; toluene-d_8): ^1H (101 °C) $\delta = 3.25$ (broad); ^1H (23 °C) $\delta = 4.06$ and 2.40 (broad, *anti*-$Mo_2(NMe_2)_4I_2$), 3.64, 2.38, and 2.25 (*gauche*-$Mo_2(NMe_2)_4I_2$); ^1H (−17 °C) $\delta = 4.06$ and 2.35 (integral ratio 1:1, *anti*), 4.04, 3.58, 2.32, and 2.29 (integral ration 1:1:1, *gauche*), *anti*/*gauche* ratio ≈ 8:2; ^{13}C (−17 °C) $\delta = 61.45$ and 43.02 (*anti*), 61.00, 58.46, 42.50, and 41.60 (*gauche*). MS (EI): $m/z = 622$ ($M^+ - H$, 3.9%), 579 ($M^+ - NMe_2$, 8.0%), 535 ($M^+ - 2NMe_2$, 13.3%), 491 ($M^+ - 3\ NMe_2$, 5.3%), 44 (NMe^+, 100%).

Preparation of $M_2(NMe_2)_5I$ (M = Mo, W). A 2.82-mmol sample of $M_2(NMe_2)_6$ and 2.82 mmol of $M_2(NMe_2)_4I_2$ were mixed and dissolved in 80 mL of toluene. The mixture was stirred for 6 h at room temperature, and the orange-brown solution was filtered through a fine frit. The solvent was removed *in vacuo*, and the yellow-brown product was dried under vacuum at 40 °C for 3 h. Crystalline material was obtained from a concentrated hexane/toluene solution (1:1) at −20 °C. Yield: *ca.* 5.1 mmol = 90%.

Characterization Data for $W_2(NMe_2)_5I$. Properties: orange-brown crystals, soluble in toluene and THF and slightly soluble in saturated hydrocarbons; mp > 180 °C dec. Anal. Calcd for $C_{10}H_{30}IN_5W_2$ (M_r 714.75): C, 16.80; H, 4.20; N, 9,80. Found: C, 15.79; H, 3.92; N, 9.18. NMR data (^1H, 299.94 MHz, toluene-d_8; ^{13}C, 75.43 MHz, C_6D_6): ^1H (106 °C) $\delta = 3.40$ ($W_2(NMe_2)_6$), 3.34 (2 $N(CH_3)_2$ *syn* to I), 3.29 (2 $N(CH_3)_2$ *geminal* to I and/or $W_2(NMe_2)_4I_2$), 3.24 ($N(CH_3)_2$ *anti* to I); ^1H (22 °C) $\delta = 4.20$ (6H, proximal CH_3 of 2 $N(CH_3)_2$ *geminal* to I), 3.33 (12H, 2 $N(CH_3)_2$ *syn* to I), 3.20 (6H, $N(CH_3)_2$ *anti* to I), 2.42 (6H, distal CH_3 of 2 $N(CH_3)_2$ geminal to I); ^1H (−87 °C) $\delta = 4.34$ (proximal CH_3 of 2 $N(CH_3)_2$ *syn* to I), 4.21 (proximal CH_3 of 2 $N(CH_3)_2$ *geminal* to I), 3.92 (proximal CH_3 of $N(CH_3)_2$ *anti* to I), 2.28 (broad signal of all distal CH_3), 4.46 and 2.44 (proximal and distal CH_3 of $W_2(NMe_2)_6$), 4.14 and 2.4 (proximal and distal CH_3 of $W_2(NMe_2)_4I_2$), $W_2(NMe_2)_5I$/$W_2(NMe_2)_6$)/$W_2(NMe_2)_4I_2$ ratio ≈ 5:1:1, K(−87 °C) ≈ 25; ^{13}C (22 °C) $\delta = 61.30$ and 38.83 (proximal and distal CH_3 of 2 $N(CH_3)_2$ *geminal* to I), 50.43 (2 $N(CH_3)_2$ *syn* to I), 48.89 (broad, $N(CH_3)_2$ *anti* to I). MS (EI): $m/z = 714$ ($M^+ - H$, 24.7%), 44 (NMe_2^+, 100%).

Characterization Data for $Mo_2(NMe_2)_5I$. Properties: orange crystals, soluble in toluene and THF and slightly soluble in hexane. NMR data (^1H, 299.94 MHz, toluene-d_8; ^{13}C, 75.43 MHz, C_6D_6): ^1H (−82 °C) $\delta = 4.29$ and 2.37 (proximal and distal CH_3 of 2 $N(CH_3)_2$ *syn* to I), 4.07 and 2.36 (proximal and distal CH_3 of 2 $N(CH_3)_2$ *geminal* to I), 3.77 and 2.37 (proximal and distal CH_3 of $N(CH_3)_2$ *anti* to I), 4.37 and 2.52 ($Mo_2(NMe_2)_6$), 4.03 and 2.21 ($Mo_2(NMe_2)_4I_2$), $Mo_2(NMe_2)_5I$/$Mo_2(NMe_2)_6$/$Mo_2(NMe_2)_4I_2$ ratio ≈ 5:1:1, K(−82 °C) ≈ 25; ^1H (25 °C) $\delta = 4.09$ and 2.50 (s, 6H each, proximal and distal CH_3 of 2 $N(CH_3)_2$ *geminal* to I), 3.34 (s, 12H, 2 $N(CH_3)_2$ *syn* to I), 3.17 (s, 6H, $N(CH_3)_2$ *anti* to I), 4.06 and 2.40 ($Mo_2(NMe_2)_4I_2$), 3.40 ($Mo_2(NMe_2)_6$); ^1H (110 °C) $\delta = 3.35$ (s, 2 $N(CH_3)_2$ syn to I), 3.28 (broad, 2 $N(CH_3)_2$ *geminal* to I and/or $Mo_2[N(CH_3)_2]_4I_2$), 3.22 (s, $N(CH_3)_2$ *anti* to I), 3.40 ($Mo_2(NMe_2)_6$; ^{13}C (25 °C) $\delta = 59.05$ and 42.85 (proximal and distal CH_3 of 2 $N(CH_3)_2$ *geminal* to I), 50.85 (2 $N(CH_3)_2$ *syn* to I), 49.13 ($N(CH_3)_2$ *anti* to I).

Preparation of $W_2(NMe_2)_5Me$. A 0.022-g (1-mmol) sample of MeLi in 5 mL of THF (0.72 mL of a 1.4 M MeLi/Et_2O solution diluted with 5 mL of THF) were added to a mixture of 0.715 g (1.0 mmol) of $W_2(NMe_2)_5I$ and 0.5 mL (3.3 mmol) of TMEDA in 20 mL of toluene at room temperature over a period of 30 min. After the mixture was stirred for 2 h, the solvent was removed *in vacuo* and the orange-brown residue was extracted with 40 mL of hexane. The filtered solution was concentrated to 10 mL. Cooling to −20 °C yielded yellow and orange crystalline material ($W_2(NMe_2)_6$, $W(NMe_2)_6$, and $W_2(NMe_2)_5Me$). Successive recrystallization increased the concentration of the product in the mother liquor. Sublimation at 110 °C and 5×10^{-3} Torr also yielded $W_2(NMe_2)_5Me$ contaminated with $W_2(NMe_2)_6$ and $W(NMe_2)_6$. Yield: *ca.* 60% based on the ^1H NMR of the crude reaction mixture. NMR data (^1H, 299.94 MHz; ^{13}C, 75.43 MHz; C_6D_6): ^1H (22 °C) $\delta = 4.23$ and 2.36 (6H each, proximal and distal CH_3 of $2N(CH_3)_2$ *genimal* to $W-CH_3$), 3.33 (18H, $3N(CH_3)_2$ *vicinal* to $W-CH_3$), 1.35 (3H, $^2J(^{183}W-H) = 8.7$ Hz, $W-CH_3$); ^{13}C (22 °C) $\delta = 59.06$ and 38.21 (proximal and distal CH_3 of $2N(CH_3)_2$ *vicinal* to $W-CH_3$), 49.56 (broad, 3 $N(CH_3)_2$ *vicinal* to $W-CH_3$), 29.94 ($W-CH_3$). MS (EI): $m/z = 603$ (M^+, 100%).

Preparation of $W_2(NMe_2)_5(CH_2C_6H_5)$. A 1:1-mL (1.1-mmol) aliquot of a 1 M $ClMgCH_2C_6H_5/Et_2O$ solution was diluted with 10 mL of THF. This solution was added slowly to 0.715 g (1.0 mmol) of $W_2(NMe_2)_5I$ dissolved in 15 mL of THF. After the mixture was stirred for 5 h at room temperature, the solvent was removed *in vacuo* leaving a dark-brown residue. $W(NMe_2)_6$ and $W_2(NMe_2)_6$ were sublimed at 100–120 °C and 10^{-3} Torr. The product distilled at 140–150 °C. Yield: *ca.* 70% based on NMR of the crude reaction mixture, 0.31 g (0.46 mmol) = 46% isolated.

---

(13) Chisholm, M. H.; Cotton, F. A.; Extine, M.; Stults, B. R. *J. Am. Chem. Soc.* **1976**, *98*, 4477.

(14) Chisholm, M. H.; Cotton, F. A.; Frenz, B. A.; Reichert, W. W.; Shive, L. W.; Stults, B. R. *J. Am. Chem. Soc.* **1976**, *98*, 4469.

(15) Bates, R. B.; Ogle, C. A. *J. Organomet. Chem.* **1982**, *47*, 3949.

(16) Rausch, M. D.; Ciappenelli, D. J. *J. Organomet. Chem.* **1967**, *10*, 127.

Properties; yellow orange oil. NMR data (^1H, 299.94 MHz; ^{13}C, 75.43 MHz, toluene-d_8): ^1H (97 °C) δ = 7.2–6.7 ($W–CH_2–C(CH)_5$), 3.59 ($W–CH_2–Ph$), 3.41 (3 $N(CH_3)_2$ *vicinal* to benzyl group), 3.40 ($2N(CH_3)_2$ *geminal* to benzyl group); ^1H (22 °C) δ = 7.2–6.7 (5H, $W–CH_2C(CH)_5$), 4.21 and 2.12 (6H each, proximal and distal CH_3 of $2N(CH_3)_2$ *geminal* to benzyl group), 3.64 (2H, $^2J(^{183}W–H)$ = 12.1 Hz, $W–CH_2–Ph$), 3.38 (18H, $3N(CH_3)_2$ *vicinal* to benzyl group); ^{13}C (22 °C) δ = 148.26 ($W–CH_2–C(CH)_5$), 128.30, 128.25, and 122.54 ($W–CH_2C(CH)_5$), 59.53 and 40.60 (proximal and distal CH_3 of $2N(CH_3)_2$ *geminal* to benzyl group), 55.87 ($J(^{183}W–^{13}C)$ = 91.4 Hz, $W–CH_2–Ph$), 49.54 ($3N(CH_3)_2$ *vicinal* to benzyl group).

Preparation of $W_2(NMe_2)_5CH_2(C_6H_4CH_3)$. A 0.144-g (1.0-mmol) sample of $KCH_2(C_6H_4)$-3-CH_3 dissolved in 15 mL of THF was added to a solution of 0.715 g (1.0 mmol) of $W_2(NMe_2)_5I$ in 20 mL of THF. A white precipitate formed. The mixture was stirred for 5 h at room temperature. The solvent was removed *in vacuo* and the brown residue extracted with 30 mL of hexane. The hexane solution was concentrated to dryness, and the residue was distilled using a kugelrohr oven. The product was collected at 120 °C and 10^{-3} Torr. Yield: 0.4 g (0.58 mmol) = 58%.

Properties: yellow-orange oil, soluble in hydrocarbons and ethers. NMR data (^1H, 299.95 MHz; ^{13}C, 75.43 MHz; C_6D_6): ^1H (50 °C) δ = 7.2–6.6 (m, $CH_2(C_6H_4)CH_3$), 4.22 and 2.12 (broad, proximal and distal CH_3 of $2N(CH_3)_2$ *geminal* to xylyl group), 3.69 (s, $CH_2(C_6H_4)CH_3$) 3.38 (s, $2N(CH_3)_2$ *syn* to xylyl group), 3.37 ($N(CH_3)_2$ *anti* to xylyl group), 2.14 (s, $CH_2(C_6H_4)CH_3$); ^1H (23 °C) δ = 7.2–6.6 (m, 4H, $CH_2(C_6H_4)CH_3$), 4.22 and 2.12 (s, 6H each, proximal and distal CH_3 of $2N(CH_3)_2$ *geminal* to xylyl group), 3.74 ($^2J(^{183}W–H)$ = 12 Hz, s, 2H, $CH_2(C_6H_4)CH_3$), 3.38 (broad, s, 18H, $3N(CH_3)_2$ *vicinal* to xylyl group), 2.15 (s, 3H, $CH_2(C_6H_4)CH_3$); ^{13}C (23 °C) δ = 148.0 and 137.5 ($CH_2C(CH)_4CCH_3$), 128.93, 128.03, 125.39, and 123.30 ($CH_2C(CH)_4CCH_3$), 59.51 and 40.77 (proximal and distal CH_3 of $2N(CH_3)_2$ *geminal* to xylyl group), 55.86 ($CH_2(C_6H_4)CH_3$), 49.49 (broad, $3N(CH_3)_2$ *vicinal* to xylyl group), 21.65 ($CH_2(C_6H_4)CH_3$). MS (EI): *m/z* = 692 ($M^+ - H$, 57.9%), 45 ($HNMe_2^+$, 100%).

Preparation of $Mo_2(NMe_2)_5CH_2(C_6H_5)$. A 1.08-g (2.0-mmol) sample of $Mo_2(NMe_2)_5I$ and 0.7 g (4.0 mmol) of TMEDA were dissolved in 20 mL of toluene. To this mixture was added 0.14 g (2.21 mmol; 1.3 mL 1.7 M/pentane) of Li^tBu in 10 mL of toluene during 1 h at room temperature. The dark-brown solution was stirred for an additional hour. The solvent was removed *in vacuo* and the brown oily residue extracted with 30 mL of hexane. Removal of the hexane yielded a crude reaction product that was purified by fractional distillation with a kugelrohr oven at ca. 120 °C at 10^{-2} Torr. Yield: 0.3 g (0.60 mmol) = 30%.

Properties: yellow-orange oil, soluble in all standard solvents. NMR data (^1H, 299.94 MHz; ^{13}C, 75.43 MHz; toluene-d_8): ^1H (23 °C) δ = 7.1–6.7 (m, 5H, $CH_2(C_6H_5)$), 4.12 and 2.15 (s, 6H each, proximal and distal CH_3 of $2N(CH_3)_2$ *geminal* to benzyl group), 3.72 (s, 2H, $CH_2(C_6H_5)$), 3.37 (s, 12H, 2 $N(CH_3)_2$ *syn* to benzyl group), 3.32 (s, 6H, $N(CH_3)_2$ *anti* to benzyl group); ^1H (−87 °C) δ = 7.2–6.8 (m, $CH_2(C_6H_5)$), 4.23 and 2.50 (proximal and distal CH_3 of $2N(CH_3)_2$ *syn* to benzyl group), 4.17 and 2.09 (s, proximal and distal CH_3 of $2N(CH_3)_2$ *geminal* to benzyl group), 4.12 and 2.59 (s, proximal and distal $N(CH_3)_2$ *anti* to benzyl group), 3.88 (s, $CH_2(C_6H_5)$); ^{13}C (23 °C) δ = 149.09 ($CH_2C(CH)_5$), 128.12, 127.36, and 121.70 ($CH_2C(CH)_5$), 57.06 and 42.97 (proximal and distal CH_3 of $2N(CH_3)_2$ *geminal* to benzyl group), 50.40 ($N(CH_3)_2$ *anti* to benzyl group), 49.76 ($2N(CH_3)_2$ *syn* to benzyl group), 45.25 ($CH_2(C_6H_5)$).

Preparation of $W_2(NMe_2)_4(CH_2SiMe_3)I$. To a solution of 1.0 g (1.40 mmol) of $W_2(NMe_2)_5I$ in 15 mL of toluene were added 1 mL of TMEDA and then a solution of 0.14 g (1.49 mmol) of $LiCH_2SiMe_3$ in 8 mL of THF over a period of 15 min. After the mixture was stirred for 2 h, the solvents were exchanged against 20 mL of hexane and the insoluble residue filtered off. The hexane was removed under reduced pressure. Yield: 0.8 g contaminated with $W_2(NMe_2)_6$. The crude reaction product was redissolved in 25 mL of toluene and a solution of 0.35 g (1.75 mmol) of Me_3SiI in 10 mL of toluene was added. After the mixture was stirred for 3 h, all volatile material was removed *in vacuo*. The crude reaction product was distilled at 130–140 °C and 10^{-3} Torr. Due to decomposition during distillation, only a small amount of oily orange $W_2(NMe_2)_4(CH_2SiMe_3)I$ was obtained.

NMR data for $W_2(NMe_2)_5(CH_2SiMe_3)$ (^1H, 299.94 MHz; ^{13}C, 75.43 MHz, C_6D_6): ^1H (23 °C) δ = 4.25 (s, proximal CH_3 of $2N(CH_3)_2$ *geminal* to CH_2SiMe_3), 3.30 (s, $2N(CH_3)_2$ *syn* to CH_2SiMe_3), 2.48 (s, distal CH_3 of $2N(CH_3)_2$ *geminal* to CH_2SiMe_3), 1.31 ($^2J(^{183}W–H)$ = 11.32 Mz, s, CH_2SiMe_3), 0.20 (s, $CH_2Si(CH_3)_3$); ^{13}C (23 °C) δ = 59.76 and 38.77 (proximal and distal CH_3 of $2N(CH_3)_2$ *geminal* to CH_2SiMe_3), 49.67 ($3N(CH_3)_2$ *vicinal* to CH_2SiMe_3), 36.87 (CH_2SiMe_3), 3.32 ($CH_2Si(CH_3)_3$). NMR data for $W_2(NMe_2)_4(CH_2SiMe_3)I$ (^1H, 299.95 MHz; ^{13}C, 75.43 MHz; toluene-d_8): ^1H (−38 °C) δ = 4.4–3.8 and 2.6–2.0 (m, proximal and distal $N(CH_3)_2$), 1.56 (d) and 0.95 (d) ($^2J(HH)$ = 12.9 Hz, CH_2SiMe_3), 0.23 (s, $CH_2Si(CH_3)_3$).

Preparation of $Mo_2(NMe_2)_4(CH_2(C_6H_5))(CH_2SiMe_3)$. To a solution of 0.25 g (0.5 mmol) of $Mo_2(NMe_2)_5CH_2(C_6H_5)$ in 10 mL of toluene was added 0.2 mL (0.5 mmol) of a 2.5 M solution of Me_3SiI in toluene. After the mixture was stirred for 20 h, 0.2 mL of TMEDA was added followed by 0.53 mL of a 1.0 M solution of $LiCH_2SiMe_3$ in pentane. After the mixture was stirred for an additional 4 h, the solvents were removed under reduced pressure and the brown residue was extracted with 10 mL of hexane. Evaporation of the hexane yielded a brown oil. Upon distillation a yellow-orange oil was collected at 130 °C and 10^{-3} Torr. There was just enough product for NMR and MS characterization.

Properties: yellow-orange oil, soluble in hexane and toluene. NMR data (^1H, 299.95 MHz; ^{13}C, 75.43 MHz, toluene-d_8): ^1H (−67 °C): δ = 7.17–6.8 (m, $CH_2(C_6H_5)$), 4.16, 4.02, 3.94, and 3.93 (s, proximal CH_3 of 4 different $N(CH_3)_2$), 2.53, 2.52, 2.26, and 1.96 (s, distal CH_3 of 4 different $N(CH_3)_2$), 3.82 (d) and 3.44 (d) ($^2J(HH)$ = 11.3 Hz, $CH_2(C_6H_5)$), 1.64 (d) and 1.24 (d) ($^2J(HH)$ = 12.5 Hz, CH_2SiMe_3), 0.23 (s, $CH_2Si(CH_3)_3$); ^{13}C (−67 °C) δ 148.08, 128.02, 127.48, and 121.68 ($CH_2(C_6H_5)$), 56.60 (broad), 42.74 and 38.88 ($N(CH_3)_2$), 47.01 ($CH_2(C_6H_5)$), 27.83 (CH_2SiMe_3), 3.27 ($CH_2Si(CH_3)_3$. MS (EI): *m/z* = 546 (M^+, 0.5%), 92 (CH_2Ph^+), 55%), 73 ($SiMe_3^+$, 100%), 44 (NMe_2^+, 28%), 587 ($Mo_2(NMe_2)_4(CH_2Ph)I$, 0.3%).

Preparation of $W_2(NMe_2)_5PPh_2$. A 0.5-mL (3.3-mmol) aliquot of TMEDA was added to a solution of 0.715 g (1.0 mmol) of $W_2(NMe_2)_5I$ in 20 mL of toluene. To this mixture was added 0.20 g (1.1 mmol) of $LiPPh_2$ in 10 mL of THF over a period of 30 min at room temperature ($LiPPh_2$ was prepared from $HPPh_2$ and BuLi in hexane). After the mixture was stirred for 2 h, the solvent was removed *in vacuo* and the dark-brown residue was extracted with 40 mL of hexane. The orange hexane solution was concentrated to dryness, leaving an orange-brown solid. $W_2(NMe_2)_6$ and $W(NMe_2)_6$ were sublimed at 100–120 °C and 10^{-3} Torr. Increasing the temperature to 140–150 °C yielded pure product. Yield: 0.45 g (0.58 mmol) = 58%.

Properties: orange crystals, soluble in hexane, toluene, and THF, which are air stable for several hours; mp 174 °C. Anal. Calcd for $C_{22}H_{40}N_5PW_2$ (M_r 773.14): C, 34.17; H, 5.17, N, 9.06. Found: C, 33.85; H, 5.16; N, 8.60. NMR data (^1H, 299.94 MHz; ^{13}C, 75.43 MHz; ^{31}P, 146.16 MHz): ^1H (76 °C, C_6D_6) δ = 7.9–6.9 (10H, $P(C_6H_5)_2$, 3.36 (12H), and 3.34 (6H) ($3N(CH_3)_2$ *vicinal* to PPh_2), 3.21 (12H, $2N(CH_3)_2$ *geminal* to PPh_2); ^1H (23 °C, C_6D_6) δ = 7.9–6.9 (10H, $P(C_6H_5)_2$), 3.32 (30H, broad, $5N(CH_3)_2$); ^1H (−88 °C, toluene-d_8) δ = 8.1–6.8 ($P(C_6H_5)_2$), 4.28, 4.22, 2.44, and 2.12 (proximal and distal CH_3 of $2N(CH_3)_2$ *geminal* and $2N(CH_3)_2$ *vicinal* to PPh_2), 4.13 and 2.42 (proximal and distal CH_3 of $N(CH_3)_2$ *anti* to PPh_2); ^{13}C (76 °C, C_6D_6) δ = 144.13 ($P(C(CH)_5)_2$, 134.61, 134.41, and 125.99 ($P(C(CH)_5)_2$), 50.45 ($2N(CH_3)_2$ *syn* to PPh_2), 49.67 ($N(CH_3)_2$ *anti* to PPh_2), 49.32 ($2N(CH_3)_2$ *geminal* to PPh_2); ^{31}P (23 °C, toluene-d_8) δ = 74.38 ($J(^{183}W–^{31}P)$ = 234.5 Hz). MS (EI): *m/z* = 773 (M^+, 0.4%); 44 (NMe_2^+, 100%).

Preparation of $W_2(NMe_2)_4(Fe(C_5H_4)_2)$. A solution of 0.43 g (1.0 mmol) of $[Li_2(TMEDA)]_2[Fe(C_5H_4)_2]$ in 10 mL of Et_2O/THF (1:1) was added to a solution of 1.43 g (2.0 mmol) of $W_2(NMe_2)_5I$ in 20 mL of toluene slowly at room temperature. After the mixture was stirred for 12 h, the solvent was removed and the brown residues extracted with 30 mL of hexane. The hexane was also removed, and the residue was heated to *ca.* 120 °C in a dynamic vacuo (10^{-3} Torr). After 4 h all of the $W_2(NMe_2)_6$ had sublimed. The residue was extracted with 20 mL of hexane. The red solution was concentrated to *ca.* 5 mL. When the solution was cooled to −20 °C, red crystals were formed. Yield: 0.25 g (0.35 mmol) = 35%.

Properties: dark red crystals, soluble in hydrocarbons and THF. NMR data (^1H, 299.94 MHz; ^{13}C, 75.43 MHz; toluene-d_8): ^1H (−58 °C) δ = 5.05, 4.82, 4.76, and 4.03 (s, 2H each, $Fe(C_5H_4)_2$), 4.33, 4.18, 2.57, and 2.23 (s, 6H each, proximal and distal $N(CH_3)_2$); ^{13}C (−68 °C) δ = 112.08 ($C(C_4H_4)$), 83.22, 76.31, 74.67, and 71.18 ($C(C_4H_4)$), 61.75, 57.30, 40.26, and 36.17 ($N(CH_3)_2$). MS (EI): *m/z* = 726 (M^+, 33%), 186 ($FeCp_2^+$, 100%).

Crystallographic Studies. General operating procedures have been given previously along with a listing of programs.[17] A summary of crystal data is given in Table I and for the sake of space in the journal the specific details of each structural determination and the modeling of the disordering

---

(17) Chisholm, M. H.; Folting, K.; Huffman, J. C.; Kirkpatrick, C. C. *Inorg. Chem.* **1984**, *23*, 1021.

have been placed in the supplementary material except for $W_2I(NMe_2)_5$ and $W_2(NMe_2)_4(\mu\text{-}(C_5H_4)_2Fe)$, which are discussed below.

$W_2I(NMe_2)_5$. A crystal of suitable size was mounted in a nitrogen atmosphere glove bag using silicone grease, and it was then transferred to a goniostat where it was cooled to −170 °C for characterization and data collection. A systematic search of a limited hemisphere of reciprocal space revealed intensities having primitive orthorhombic symmetry. Following complete intensity data collection, systematic absences limited the space group to *P*2~1~*nb* or *Pmnb*. After correction for absorption, data processing gave a residual of 0.057 for the averaging of 795 unique intensities which had been measured more than once. Four standards measured every 300 data showed no significant trends.

The structure was solved using a combination of direct methods (SHELXS-86), least-squares refinement, and Fourier techniques. Actually an attempt was made to solve the structure in both of the above space groups. In each case the W and I positions were obtained from an *E*-map. The remaining non-hydrogen atoms were determined from subsequent iterations of least-squares refinement and difference Fourier calculation. When space group $P2_1nb$ was used, the isotropic thermal parameters ranged from 0.0 to 9.6 Å^2 and several of the bonds and angles converged to abnormal values. All of these parameters were much better behaved when space group *Pmnb* was used, and therefore it was taken to be the correct space group. In the later stages of refinement, two persistent peaks of about 3 e/Å^3 were observed in the difference maps in the direction of the W(2)–N(7) and W(2)–N(10) bonds, just slightly longer than the W–I bond. These were assumed to be disordered iodines, and their occupancies were refined giving values of about 5%. These occupancies were then fixed for the remainder of the refinement. Hydrogens were not observed in the difference maps and since several of the methyl groups were near the disorder, no attempt was made to include them.

In the final cycles of refinement, the disordered iodines were varied with isotropic thermal parameters and all other atoms were varied with anisotropic thermal parameters to a final $R(F) = 0.047$. The largest peaks in the final difference map were tungsten residuals of 1.8–2.0 e/Å^3. All other peaks were 1.0 e/Å^3 or less. The largest hole was −1.3 e/Å^3.

Atoms I(3), W(1), W(2), N(7), C(8), C(9), and I(14) all lie in a crystallographic mirror plane, with the remaining atoms being symmetry related above and below the plane.

$W_2(NMe_2)_4(Fe(C_5H_4)_2)$. The space group is $P\bar{1}$ with two independent molecules in the asymmetric unit. The two molecules are almost identical as shown by the best molecular fit, *however*, they are neither "*lined up*" with each other in the unit cell, *i.e.* related by some translation, nor related by other symmetry elements. Studies of unit cell packing diagrams using CERIUS (Molecular Modelling) did not reveal any additional relationships between the molecules, other than the centers of inversion and unit cell translations.

The full unique data set was sorted according to $(\sin\theta)/\lambda$ and there was no evidence of equivalent reflections, indicating overlooked symmetry.

All of the crystals examined looked twinned; i.e., they had a definite dividing line, relating similar halves. It was possible to cleave the crystal under the microscope and arrive at a single crystal. The possibility of the presence of a tiny fragment of the twin cannot be excluded and might explain the rather high *R* for the averaging of equivalent reflections.

Acknowledgment. We thank the National Science Foundation for support, and H.S. thanks the Alexander von Humboldt Foundation for a Feodor Lynen Fellowship.

Supplementary Material Available: Text describing the structure determination, tables giving anisotropic thermal parameters and complete listings of bond distances and bond angles, and VERSORT drawings (42 pages). See any current masthead for ordering information.